

Supporting Information for

Effect of the length of bromoalkyl chains on light-driven hydrogen evolution facilitated by fluorene-based polymers

Han-Sheng Sun,^{‡[a]} Tien-Liang Tsai,^{‡[a]} Cheng-Hao Chang,^[a] Yen-Yu Chen,^[a] Hau-Ren Yang,^[a] Jeffrey C.S. Wu,^{[b]} and Yu-Ying Lai^{*[a]}*

[a] Institute of Polymer Science and Engineering, National Taiwan University, Taipei, 10617, Taiwan; [b] Department of Chemical Engineering, National Taiwan University, Taipei 10617, Taiwan

Contents

1. General remarks.....	1
2. Chemical structures of PF ₈ BT and PSO	3
3. Synthetic schemes.....	3
4. Synthetic details.....	5
5. Water contact angle.....	9
6. Photoelectron spectra.....	11
7. DFT calculations.....	12
8. Mass spectra	16
9. Photocatalytic hydrogen evolution reaction	18
10. Comparison of PF ₂ SO and PF ₂ BT with their analogues in terms of HER rate	21
11. NMR spectra	22
12. IR spectra	37
13. GPC traces	39
14. Reference	41

1. General remarks

Materials.

All commercially available chemicals, which were used as received, were purchased from Sigma-Aldrich, Acros Organics, Merck Millipore and Alfa Aesar. 2-Bromoethanol¹, 2-(2-bromoethoxy)tetrahydro-2H-pyran², 2,7-dibromofluorene³, 2,2'-(2,7-dibromo-9H-fluoren-9-ylidene)bis(2,1-ethanediylloxy)]bis[tetrahydro-2H-pyran]⁴, 2,7-dibromo-9H-fluorene-9,9-diethanol⁴, 2,7-dibromo-9,9-bis(6-bromohexyl)-9H-fluorene⁵, 2,2'-[9,9-bis(6-bromohexyl)-9H-fluorene-2,7-diyl]bis[4,4,5,5-tetramethyl-1,3,2-dioxaborolane]⁶, 2,7-dibromo-9-fluorenone⁷, 3,7-dibromodibenzothiophene S,S-dioxide⁸, 4,7-dibromo-2,1,3-benzothiadiazole⁹, and phenylboronic acid pinacol ester¹⁰ were synthesized according to the reported literatures.

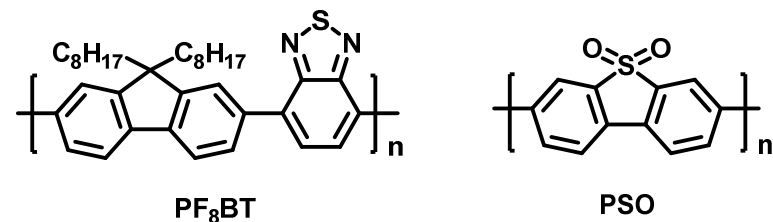
Characterization.

The ¹H and ¹³C NMR measurements were carried out by using Bruker AVIII HD 400 MHz FT-NMR. The FT-IR spectra were recorded by a PerkinElmer Spectrum Two FT-IR spectrometer. Sample pellets were made of polymer and KBr with the ratio of 3 to 100 by weight. The high-resolution mass spectra were obtained by a JEOL, JMS-700 Mass Spectrometer via fast atom bombardment method (FAB). The source accelerating voltage was operated at 10 kV with a Xe gun, using 3-nitrobenzyl alcohol (NBA) as matrix. The CHNS elemental analysis was performed by the “Elementar Vario EL cube” elemental analyzer (for NCSH, Germany). Thin-film UV-Vis absorption spectra were recorded on a Hitachi U-1900 spectrophotometer. HOMO energies were obtained by atmospheric photoelectron spectroscopy (PES) (RIKEN keiki AC2). The LUMO levels were determined from the equation : LUMO = $E_g + \text{HOMO}$. Either thin film was prepared by drop-casting a suspension of 1 mg of polymer in 1 mL of chloroform onto a 2cm × 2cm quartz substrate. Number average molecular mass (M_n) and dispersity (D) were determined with a HLC-8321GPC/HT at 160 °C with 1,2,4-trichlorobenzene as eluent using

Tosoh Bioscience LLC TSKgel GMHHR-HHT2 mixed-bed columns and narrow molecular weight distribution polystyrene standards. The residual palladium (Pd) concentration was measured by a THERMO-ELEMENT XR inductively coupled plasma-mass spectrometer (ICP-MS). Triethylamine (TEA) and acetonitrile were dehydrated by calcium hydride (CaH_2) and distilled before use.

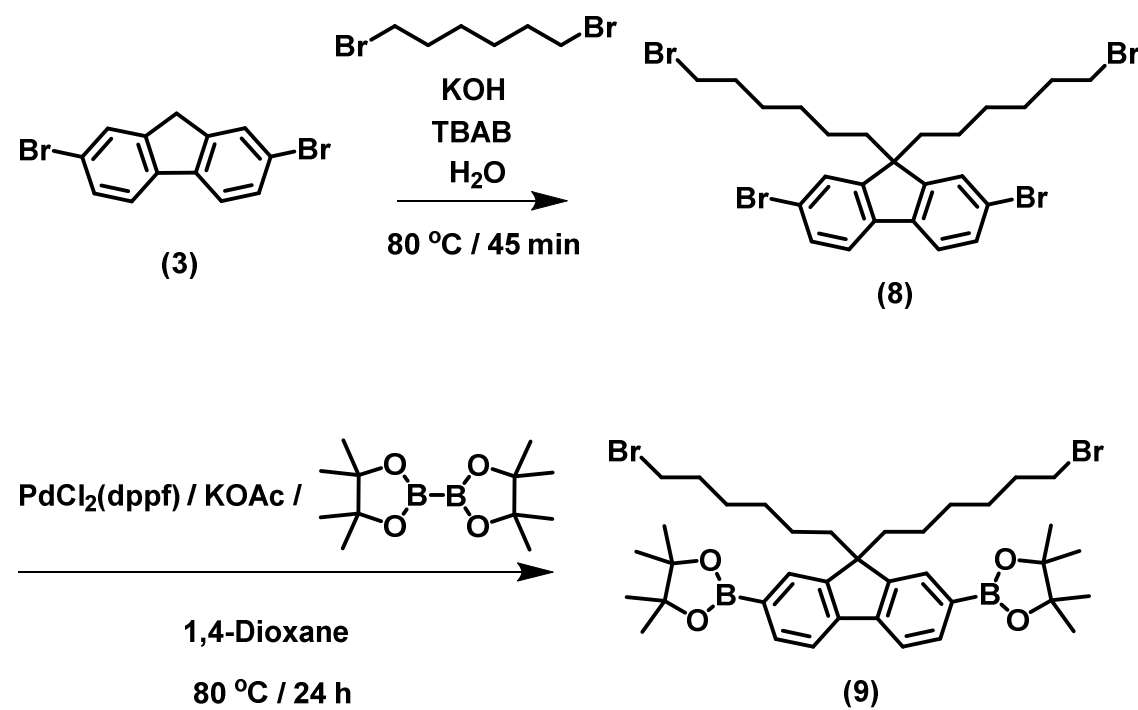
2. Chemical structures of PF₈BT and PSO

Scheme S1. Chemical structures of PF₈BT and PSO

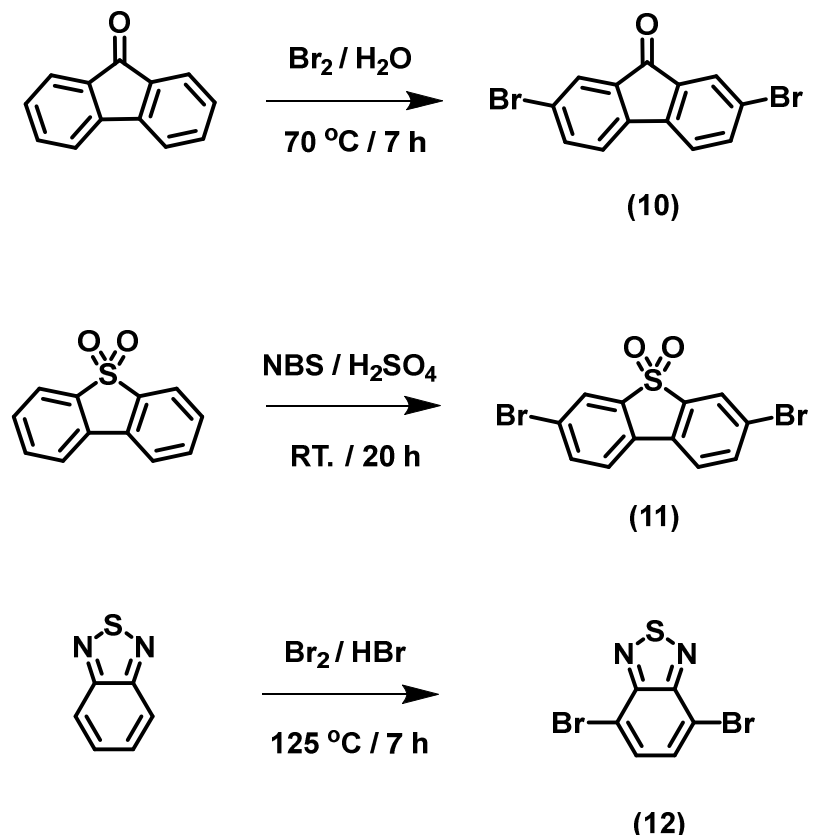


3. Synthetic schemes

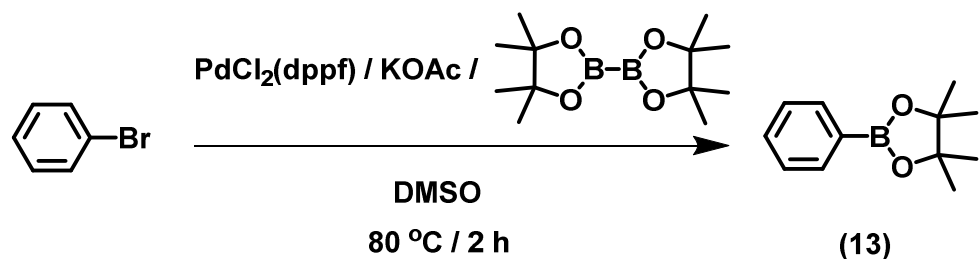
Scheme S2. Synthesis of compound **8** and **9**.



Scheme S3. Synthesis of compound **10**, **11**, and **12**.



Scheme S4. Synthesis of compound **13** for end-capping reactions on polymers



4. Synthetic details

Synthesis of 2,7-dibromo-9,9-bis(2-bromoethyl)-9H-fluorene (6).

To a solution of 2,7-dibromo-9H-fluorene-9,9-diethanol (1.50 g, 3.65 mmol) and triphenylphosphine (2.87 g, 10.95 mmol) in dry dichloromethane (40 mL), carbon tetrabromide (3.63 g, 10.94 mmol) was added dropwise at 0 °C. The reaction mixture was stirred for 16 hours at room temperature under nitrogen atmosphere, and extracted with dichloromethane. The organic phase was washed with water and brine serially, and purified by column chromatography (silica gel, hexane : dichloromethane = 6 :1) to yield 2,7-dibromo-9,9-bis(2-bromoethyl)-9H-fluorene as a white solid (1.92 g, 97.7%). ¹H NMR (400 MHz, DMSO-*d*₆, δ (ppm)): 7.98-7.97 (d, *J* = 1.7 Hz, 2H), 7.86-7.84 (d, *J* = 8.1 Hz, 2H), 7.62-7.60 (dd, *J* = 8.1 Hz, 1.8 Hz, 2H), 2.73-2.69 (m, 4H), 2.61-2.57 (m, 4H). ¹³C NMR (100 MHz, CDCl₃, δ (ppm)): 148.07, 138.75, 131.64, 126.12, 122.35, 121.77, 56.03, 42.91, and 26.23. HRMS (m/z, FAB): [M]⁺ calc. for C₁₇H₁₄⁷⁹Br₄, 533.7829; found, 533.7828.

Synthesis of 2,2'-[9,9-bis(2-bromoethyl)-9H-fluorene-2,7-diyl]bis[4,4,5,5-tetramethyl-1,3,2-dioxaborolane] (7)

A mixture of 2,7-dibromo-9,9-bis(2-bromoethyl)-9H-fluorene (1.74 g, 3.24 mmol), bis(pinacolato)diboron (2.49 g, 9.80 mmol), PdCl₂(dpff) (119.1 mg, 0.163 mmol), potassium acetate (1.92 g, 19.57 mmol), and dry 1,4-dioxane (34 mL) was degassed by freeze-pump-thaw cycles 3 times, heated at 80 °C under nitrogen atmosphere for 24 h, cooled to room temperature, evaporated under vacuum, and extracted with chloroform. The collected organic layer was washed with water and brine sequentially, purified by column chromatography (silica gel, hexane : ethyl acetate = 4 :1) and recrystallized with ethyl acetate to furnish 2,2'-[9,9-bis(2-bromoethyl)-9H-fluorene-2,7-diyl]bis[4,4,5,5-tetramethyl-1,3,2-dioxaborolane] as a yellowish solid (1.83 g, 89.6%). ¹H NMR (400 MHz, CDCl₃, δ (ppm)): 7.87-7.85 (d, *J* = 7.6 Hz, 2H), 7.81 (s, 2H), 7.74-7.72 (d, *J* = 7.6 Hz, 2H), 2.70-2.65 (m, 4H), 2.53-2.49 (m, 4H), 1.40 (s, 24H).

¹³C NMR (100 MHz, CDCl₃, δ (ppm)): 145.99, 143.42, 134.93, 128.68, 120.04, 84.05, 55.78, 43.02, 27.56, and 24.94. HRMS (m/z, FAB): [M]⁺ calc. for C₂₉H₃₈B₂⁷⁹Br₂O₄, 630.1323; found, 630.1320.

Polymerization.

Synthesis of fluorene-based Polymers.

The general procedure for synthesizing fluorene-based polymers is described as follows: To a sealed Schlenk flask were loaded dibromo monomer (1 equiv.), diboron ester monomer (1 equiv.), Pd(PPh₃)₄ (0.05 equiv.), toluene (1 mL), tetrahydrofuran (2 mL), ethanol (0.5 mL), and 2M potassium carbonate solution (1.5 mL, 17-18 equiv. of base). The mixture was degassed through freeze-pump-thaw cycles 3 times, stirred vigorously, and heated at 80 °C under nitrogen atmosphere. After 72 h, the end-capped reagents, phenylboronic acid pinacol ester and bromobenzene, were added and the reaction was continued for 12 hrs. The reaction mixture was cooled to room temperature and reprecipitated in methanol. In regular extraction, the collected solid was purified by Soxhlet extraction using methanol, acetone, hexane, and chloroform as solvent for 24 h, respectively. In extensive extraction, the collected solid was purified by Soxhlet extraction using methanol, acetone, hexane, and chloroform as solvent for 48 h, respectively.

PF₂ (107 mg, 56.8%), ¹H NMR (400 MHz, CDCl₃, δ(ppm)): 7.88-7.37 (br, protons on fluorene moiety, 6H), 2.84-2.68 (br, -CH₂CH₂Br, 8H). FT-IR (KBr, cm⁻¹): 698, 745, 817, 1221, 1257, 1406, 1438, 1454, 1523, 1569, 1604, 2855, 2924, 2966, 3007, 3028, 3055. Elem. Anal. calc. for C₁₇H₁₄Br₂ (repeating unit): C 54.00%, H 3.73%; found: C 54.93%, H 4.13%.

PF₂FO (128 mg, 38.1%), ¹H NMR (400 MHz, CDCl₃, δ (ppm)): 8.05-7.41 (br, protons on aromatic ring, 12H), 2.77-2.59 (br, -CH₂CH₂Br, 8H). FT-IR (KBr, cm⁻¹): 655, 784, 824, 1122,

1188, 1410, 1452, 1608, 1715, 2851, 2923, 3047. Elem. Anal. calc. for C₃₀H₂₀Br₂ (repeating unit): C 64.77%, H 3.62%; found: C 64.60%, H 4.00%.

PF₂SO (110 mg, 30.4%), ¹H NMR (400 MHz, CDCl₃, δ (ppm)): 8.17-7.68 (br, protons on aromatic ring, 12H), 2.81-2.65 (br, -CH₂CH₂Br, 8H). FT-IR (KBr, cm⁻¹): 576, 715, 750, 823, 1050, 1079, 1163, 1302, 1405, 1456, 1597, 2852, 2922, 3034, 3059, 3083. Elem. Anal. calc. for C₂₉H₂₀Br₂O₂S (repeating unit): C 58.80%, H 3.40%, S 5.41; found: C 58.89%, H 3.87%, S 4.90%.

PF₂BT (80 mg, 35.4%), ¹H NMR (400 MHz, CDCl₃, δ (ppm)): 8.16-7.41 (br, protons on aromatic ring, 8H), 2.89-2.75 (br, -CH₂CH₂Br, 8H). FT-IR (KBr, cm⁻¹): 511, 657, 697, 817, 1220, 1256, 1418, 1459, 1544, 1604, 2851, 2919, 2962, 3008, 3028, 3053. Elem. Anal. calc. for C₂₃H₁₆Br₂N₂S (repeating unit): C 53.93%, H 3.15%, N 5.47%, S 6.26; found: C 54.46%, H 3.48%, N 5.16%, S 6.19%.

PF₆ (174 mg, 50.0%), ¹H NMR (400 MHz, CDCl₃, δ (ppm)): 7.87-7.36 (br, protons on fluorene moiety, 6H), 3.30-3.29 (br, -CH₂CH₂CH₂CH₂CH₂CH₂Br, 4H), 2.15 (br, -CH₂CH₂CH₂CH₂CH₂CH₂Br, 4H), 1.70-1.69 (br, -CH₂CH₂CH₂CH₂CH₂Br, 4H), 1.27 (br, -CH₂CH₂CH₂CH₂CH₂Br, 4H), 1.18 (br, -CH₂CH₂CH₂CH₂CH₂Br, 4H), 0.84-0.83 (br, -CH₂CH₂CH₂CH₂CH₂Br, 4H). FT-IR (KBr, cm⁻¹): 560, 724, 754, 814, 1255, 1404, 1436, 1456, 1568, 1604, 2852, 2927, 3008, 3023, 3055. Elem. Anal. calc. for C₂₅H₃₀Br₂ (repeating unit): C 61.24%, H 6.17%; found: C 67.73%, H 6.63%.

PF₆SO (225 mg, 59.0%), ¹H NMR (400 MHz, CDCl₃, δ (ppm)): 8.19-7.35 (br, protons on aromatic ring, 12H), 3.32-3.29 (br, -CH₂CH₂CH₂CH₂CH₂CH₂Br, 4H), 2.14-2.13 (br, -CH₂CH₂CH₂CH₂CH₂CH₂Br, 4H), 1.70-1.69 (br, -CH₂CH₂CH₂CH₂CH₂Br, 4H), 1.24 (br, -CH₂CH₂CH₂CH₂CH₂Br, 4H).

CH2CH2CH2CH2CH2Br, 4H), 1.17 (br, -CH2CH2CH2CH2CH2CH2Br, 4H), 0.72 (br, -CH2CH2CH2CH2CH2CH2Br, 4H). FT-IR (KBr, cm^{-1}): 577, 716, 750, 816, 1048, 1080, 1157, 1306, 1397, 1431, 1454, 1597, 2851, 2925, 3028, 3053. Elem. Anal. calc. for C37H36Br2O2S (repeating unit): C 63.08%, H 5.15%, S 4.55; found: C 64.61%, H 5.37%, S 4.21%.

5. Water contact angle

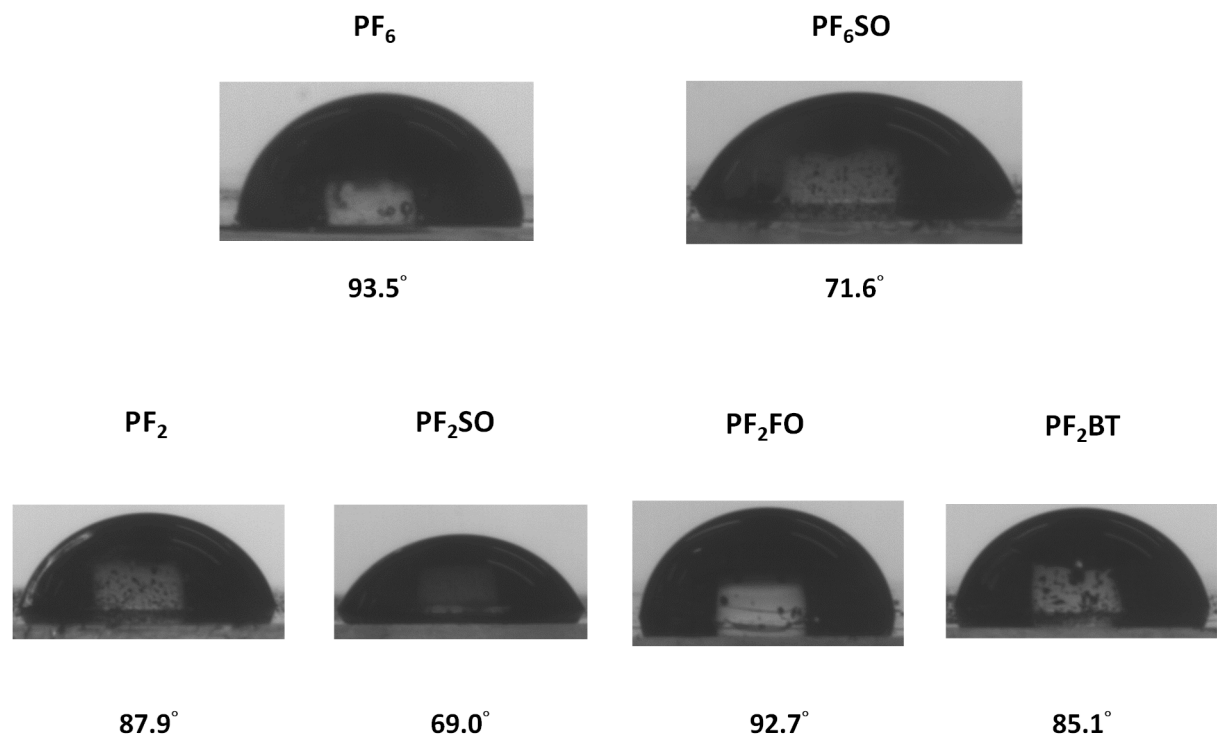


Figure S1. Water contact angles of PF_6 , PF_6SO , PF_2 , PF_2SO , PF_2FO , and PF_2BT .

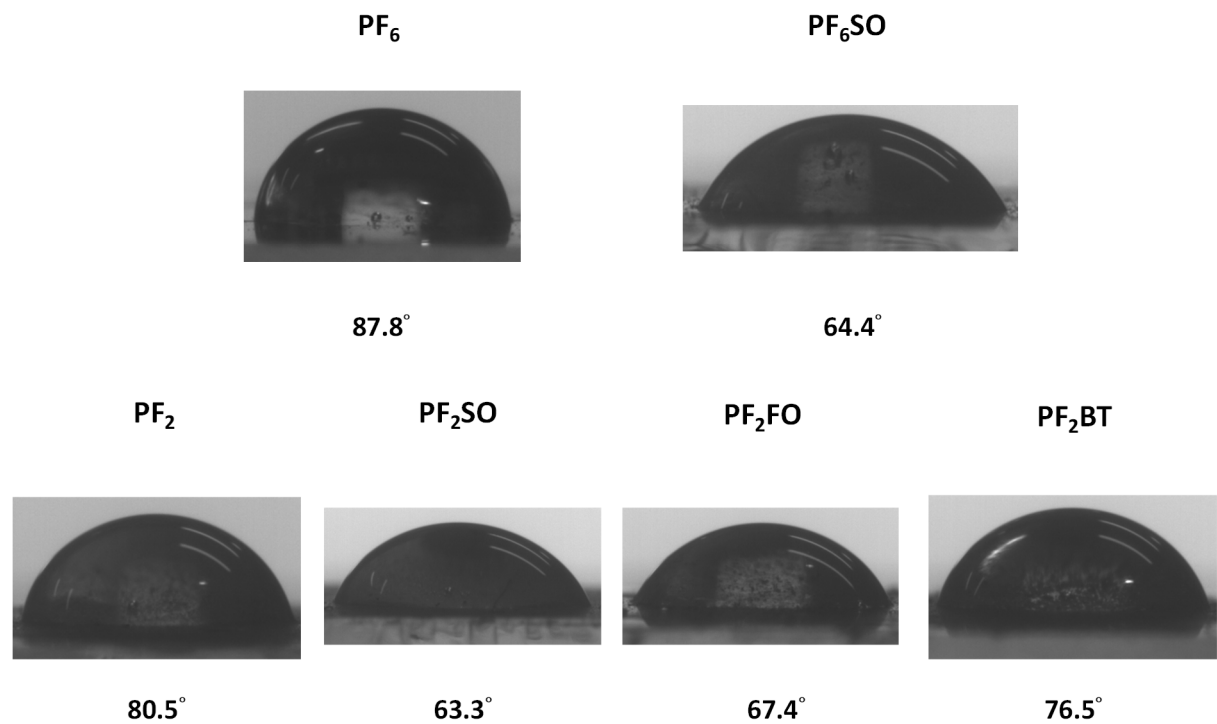


Figure S2. Water contact angles of PF_6 , PF_6SO , PF_2 , PF_2SO , PF_2FO , and PF_2BT after treating with TEA.

Table S1. Summary of water contact angles before and after treatment with TEA.

	Original WCA	WCA after treatment with TEA ^a
PF₆	93.5°	87.8°
PF₆SO	71.6°	64.4°
PF₂	87.9°	80.5°
PF₂SO	69.0°	63.3°
PF₂FO	92.7°	67.4°
PF₂BT	85.1°	76.5°

^aEach polymer thin film was treated with pure TEA. Unreacted TEA was then removed under vacuum.

6. Photoelectron spectra

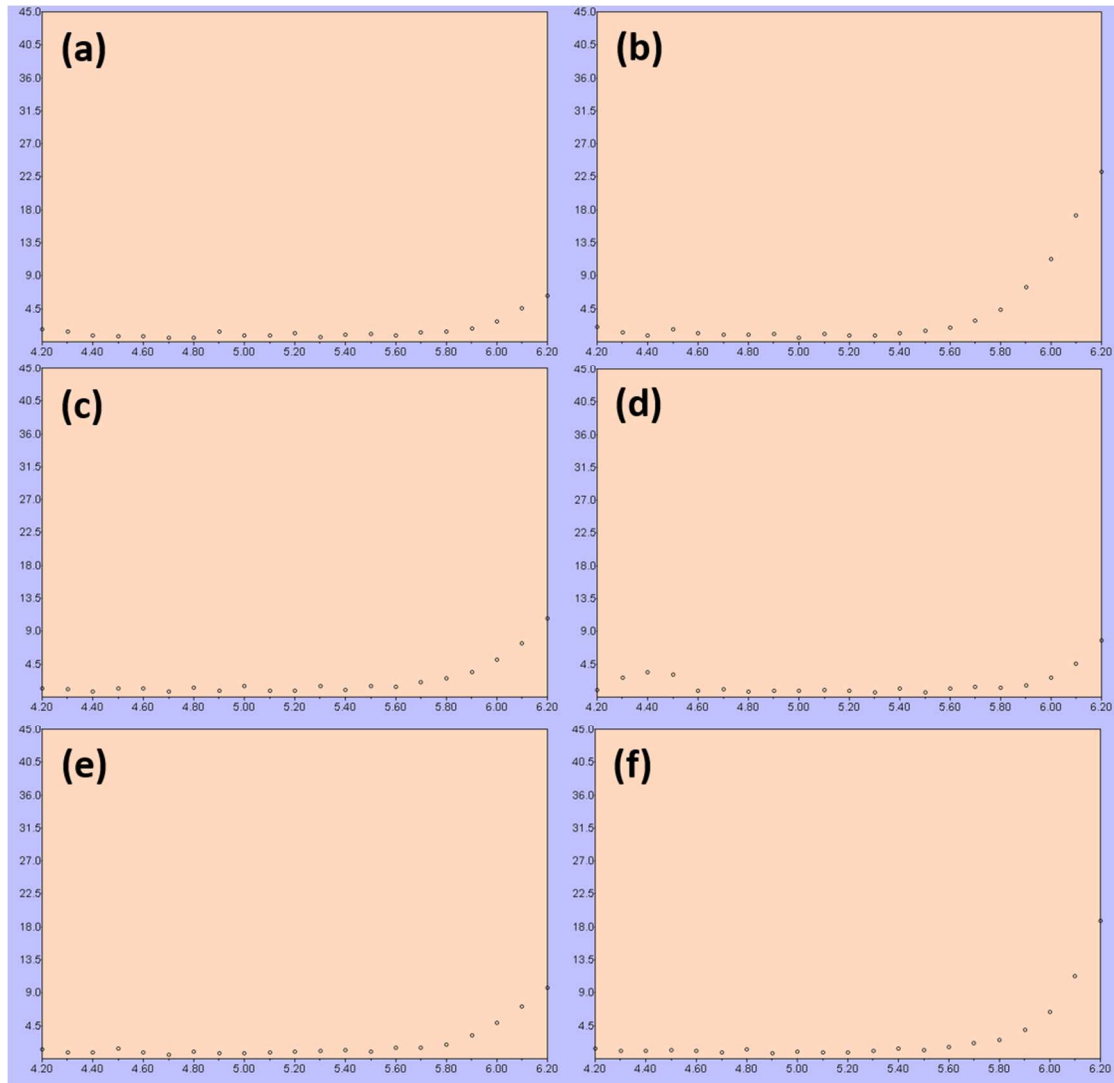


Figure S3. Atmospheric photoelectron spectra of (a) PF₂, (b) PF₂FO, (c) PF₂SO, (d) PF₂BT, (e) PF₆, (f) PF₆SO.

7. DFT calculations

Density functional theory (DFT) calculations were performed with the Gaussian09. Molecular fragments of polymers were used to model the polymers. Geometry optimization was carried out at the ω B97XD/6-311G(d,p) level of theory with solvation in chloroform by applying the SMD model. The minimum nature of each optimized structure was verified by vibrational analysis. PBE1PBE/6-311G(d,p) was then employed in time-dependent DFT (TDDFT) calculations with solvation in chloroform by applying the SMD model.

Table S2. Calculated excitation wavelength (λ_{calc}), oscillator strength, symmetry, and configuration (with largest CI coefficients) of the selected excited states.

compound	λ_{calc} (nm)	oscillator strength	symmetry	configuration
PF₂	341	2.900	Singlet-A	H-1 → L (70%)
PF₂FO	444	0.287	Singlet-A	H → L (81%)
	344	2.021	Singlet-A	H → L+2 (77%)
	294	0.583	Singlet-A	H-11 → L (38%)
PF₂SO	372	2.459	Singlet-A	H → L (91%)
	311	0.215	Singlet-A	H → L+2 (68%)
PF₂BT	441	0.857	Singlet-A	H → L (93%)
	318	0.243	Singlet-A	H-2 → L (59%)

	315	0.976	Singlet-A	H → L+2 (67%)
PF₆	347	2.887	Singlet-A	H → L (67%)
PF₆ SO	379	2.296	Singlet-A	H → L (91%)
	317	0.233	Singlet-A	H → L+2 (75%)

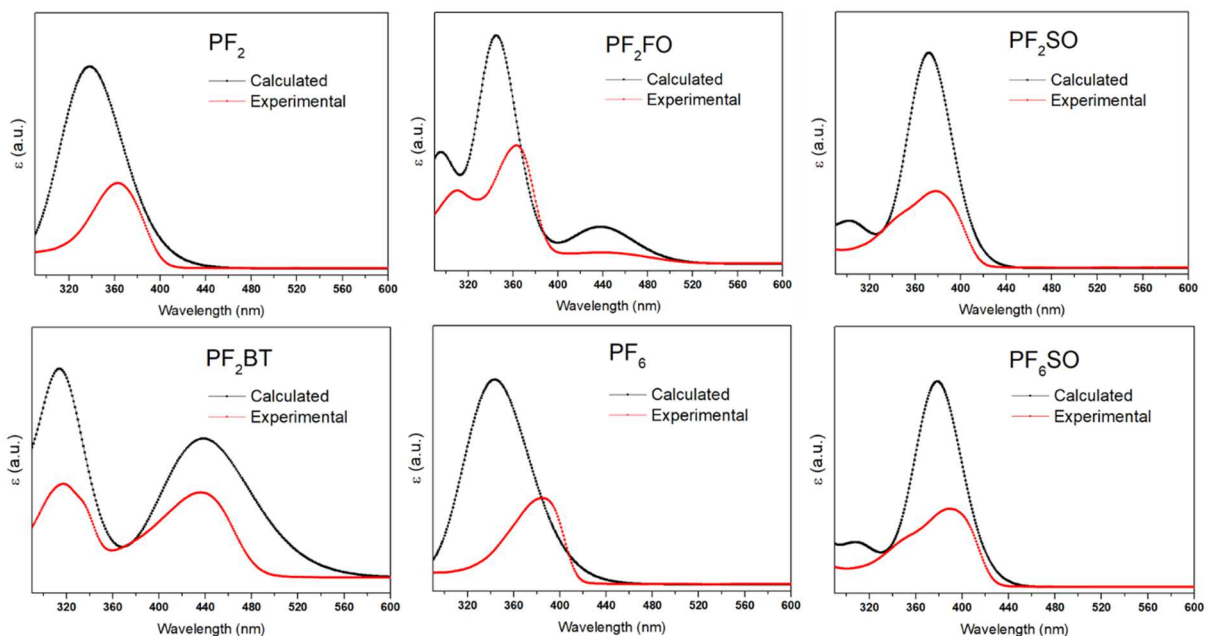
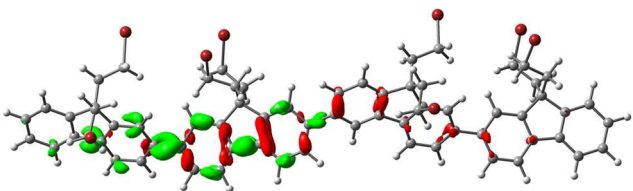
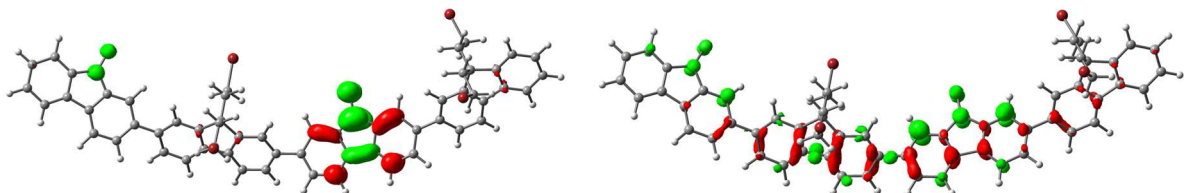
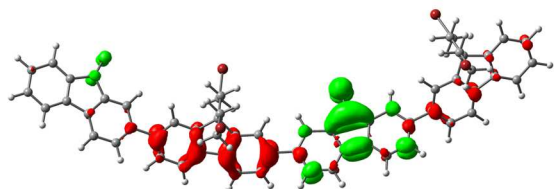
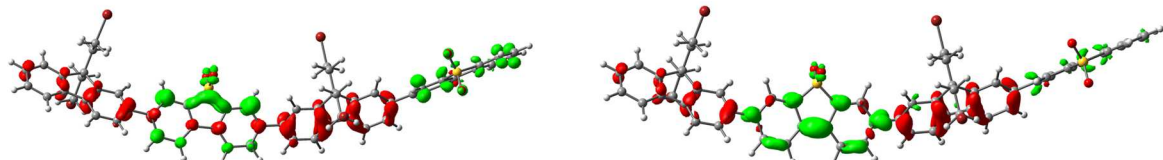
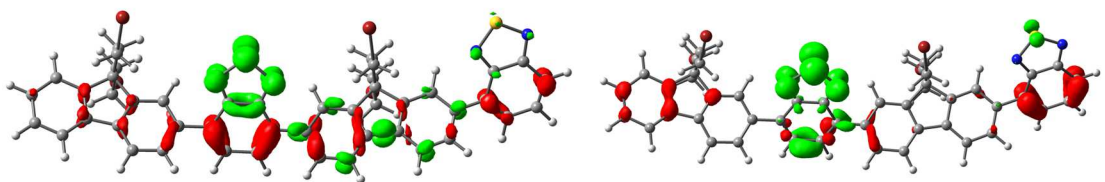
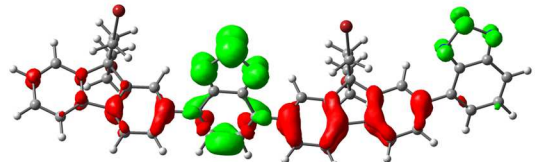


Figure S4. Experimental and calculated UV-Vis spectra. The red lines are experimental data and the black lines are calculated results.

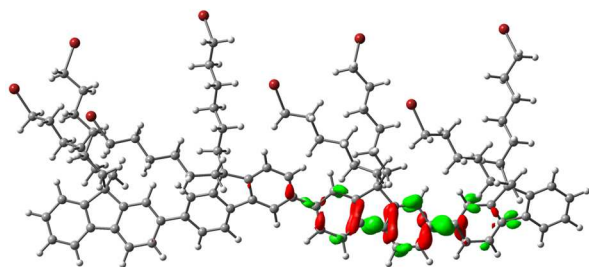
PF₂ $\lambda_{\text{calc}} = 341 \text{ nm}$

PF₂FO $\lambda_{\text{calc}} = 294 \text{ nm}$ $\lambda_{\text{calc}} = 344 \text{ nm}$  $\lambda_{\text{calc}} = 444 \text{ nm}$

PF₂SO $\lambda_{\text{calc}} = 311 \text{ nm}$ $\lambda_{\text{calc}} = 372 \text{ nm}$

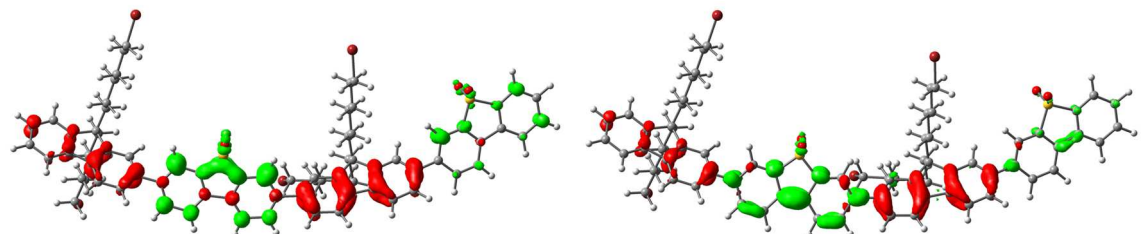
PF₂BT $\lambda_{\text{calc}} = 315 \text{ nm}$ $\lambda_{\text{calc}} = 318 \text{ nm}$  $\lambda_{\text{calc}} = 441 \text{ nm}$

PF₆



$\lambda_{\text{calc}} = 347 \text{ nm}$

PF₆SO



$\lambda_{\text{calc}} = 317 \text{ nm}$

$\lambda_{\text{calc}} = 379 \text{ nm}$

Figure S5. Changes in electron density of selected electronic transitions plotted with isovalue 0.0015 au. Red indicates a decrease in electron density, while green indicates an increase.

8. Mass spectra

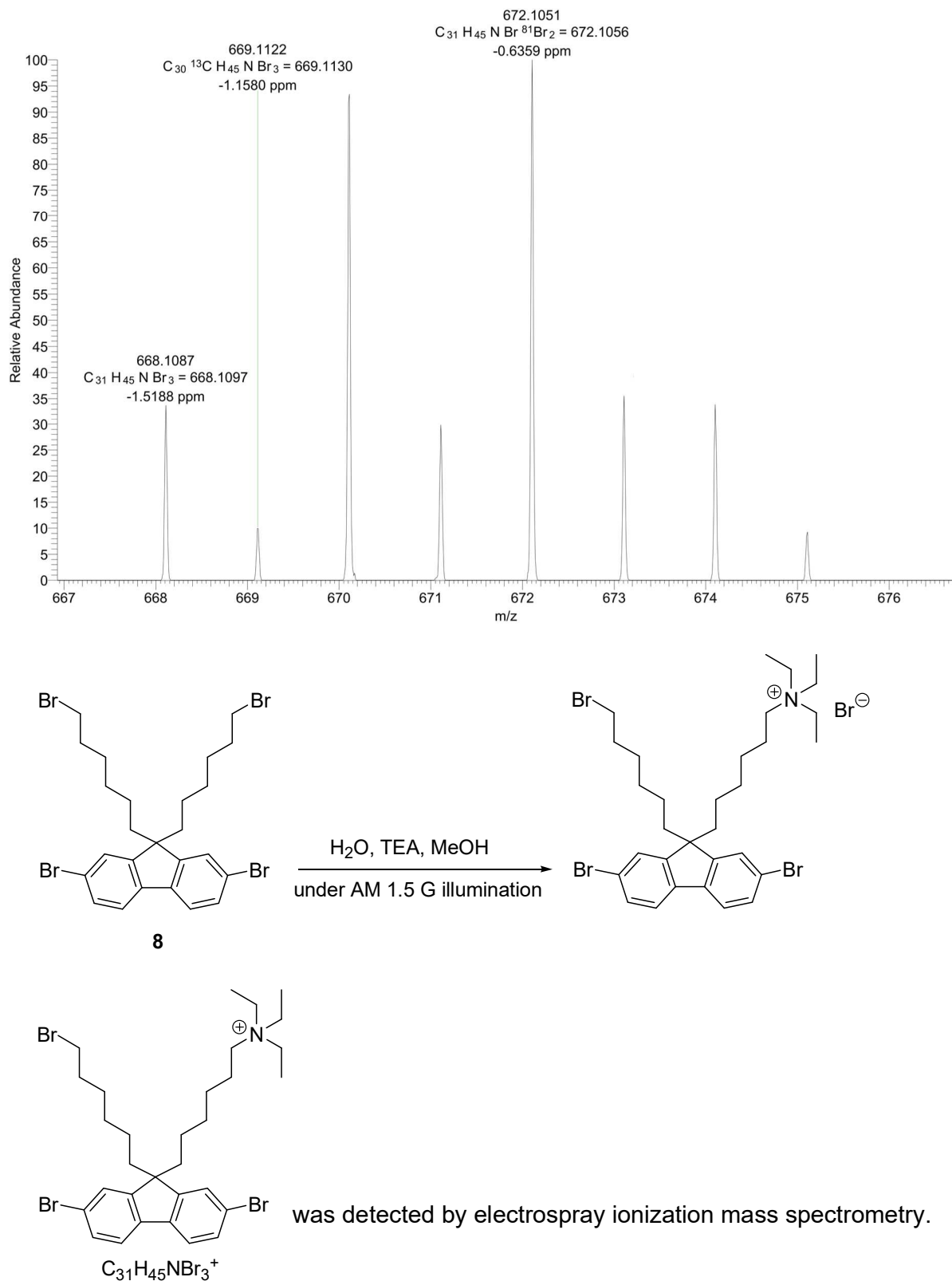


Figure S6. Detection of the formation of tetraalkylammonium group by electrospray ionization mass spectrometry.

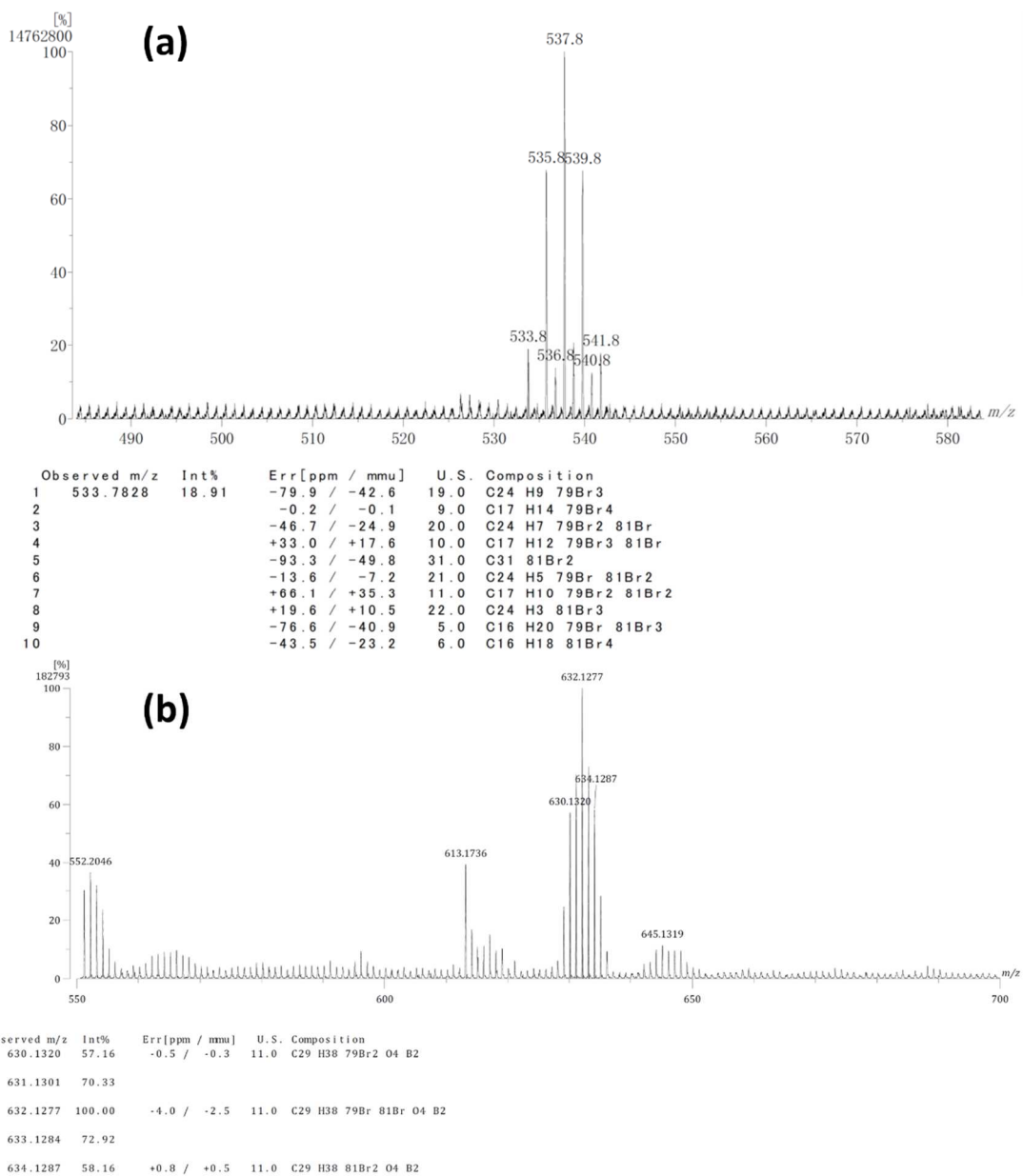
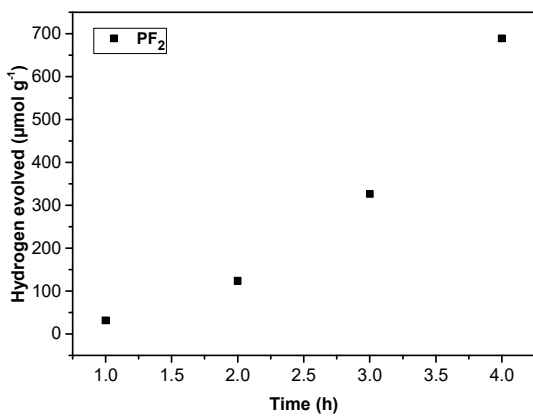


Figure S7. High resolution mass spectra of (a) 2,7-dibromo-9,9-bis(2-bromoethyl)-9H-fluorene (**6**) and (b) 2,2'-[9,9-bis(2-bromoethyl)-9H-fluorene-2,7-diyl]bis[4,4,5,5-tetramethyl-1,3,2-dioxaborolane] (**7**)

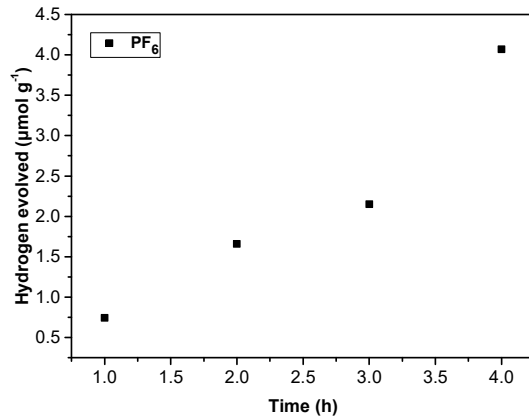
9. Photocatalytic hydrogen evolution reaction

Each photocatalytic hydrogen evolution reaction was performed in a sealed glass reactor (50 mL). Polymer (5 mg) and a solution (25 mL) of triethylamine (TEA)/methanol (MeOH)/deionized water (H₂O) (1/1/1 (v/v/v)) was added into the reactor. The mixture was stirred rapidly and purged with argon (Ar) for 15 minutes. Subsequently, the reaction system was irradiated by a 300W Xenon lamp (model 66902) equipped with an AM 1.5G filter (solar simulator: PEC-11, Peccel Technologies, Inc., Kanagawa, Japan). After 4 h, the amount of produced hydrogen was analyzed by a gas chromatograph (GC) with a thermal conductivity detector (TCD). The calibration curve based on the ideal gas law was established by using certified 0.3 vol% H₂/Ar mixture gas. The rate of hydrogen evolution is expressed in moles per gram of polymer and per hour.

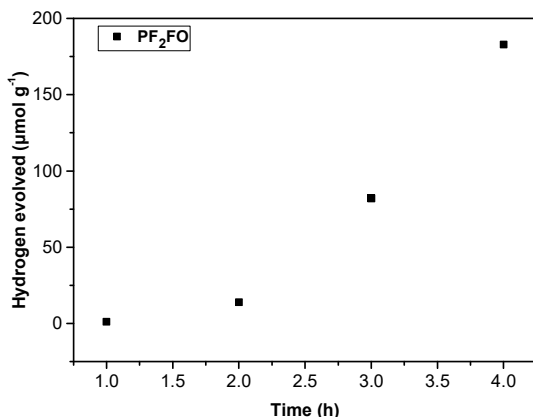
(a)



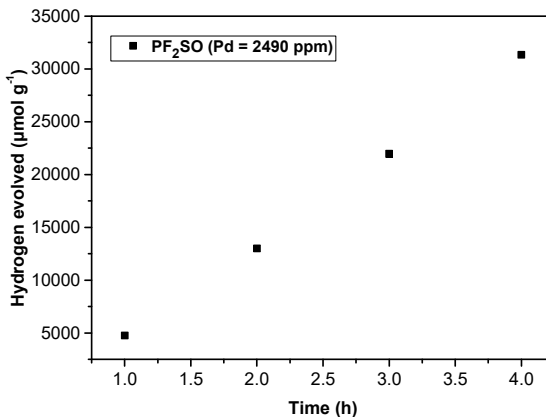
(b)



(c)



(d)



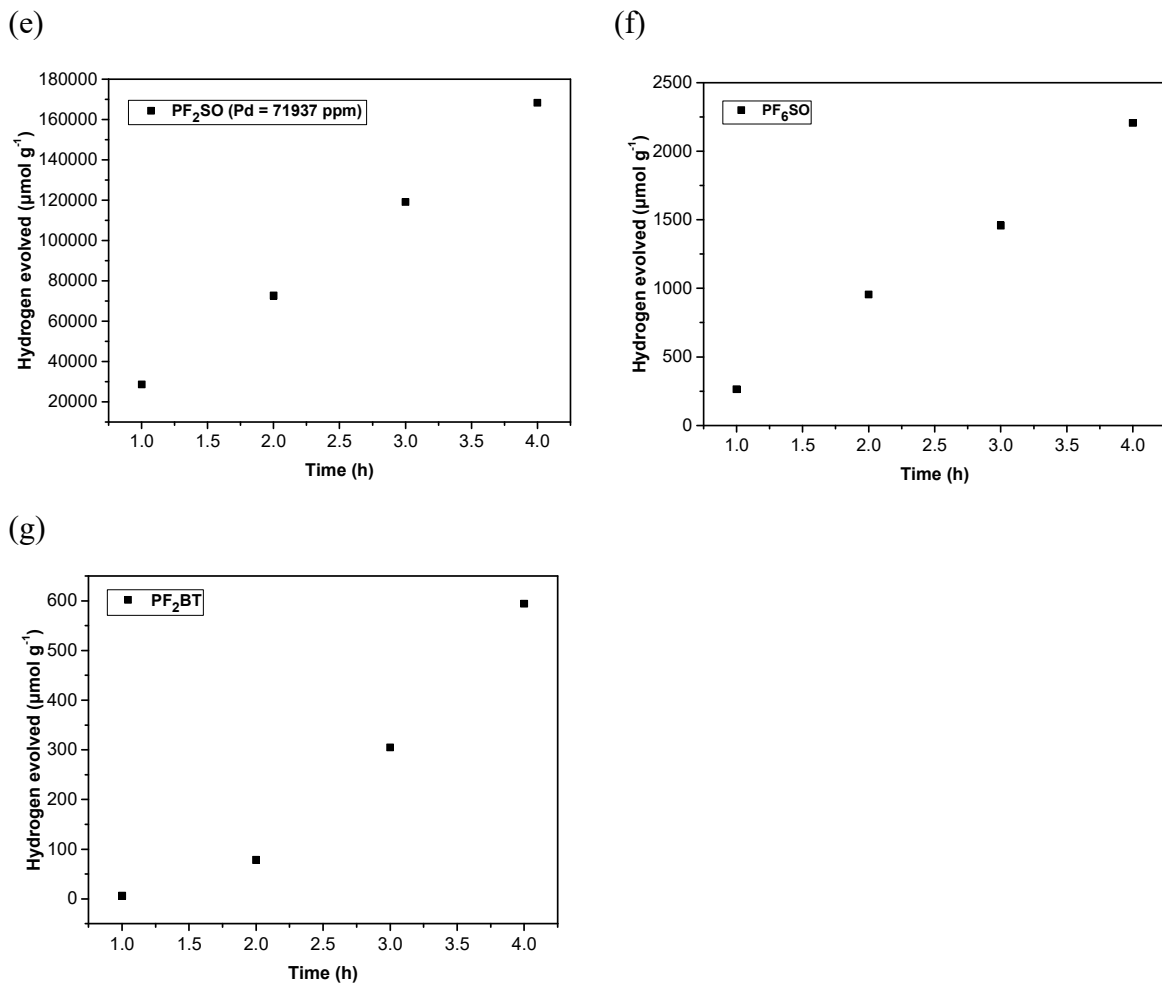


Figure S8. Time course of hydrogen evolution for all polymers.

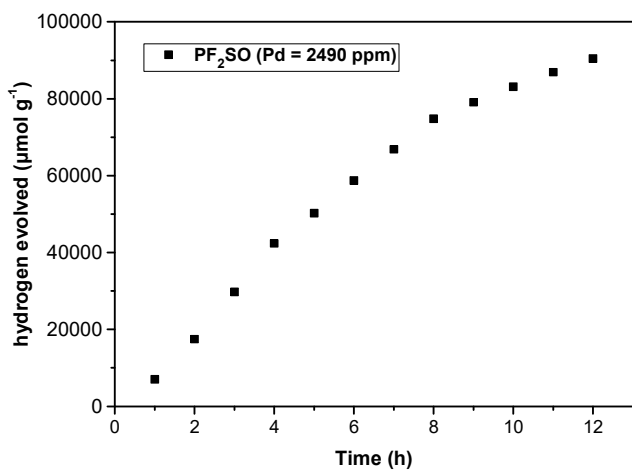


Figure S9. Hydrogen production by **PF₂SO** over a period of 12 hours in cycles of 2 hours each.

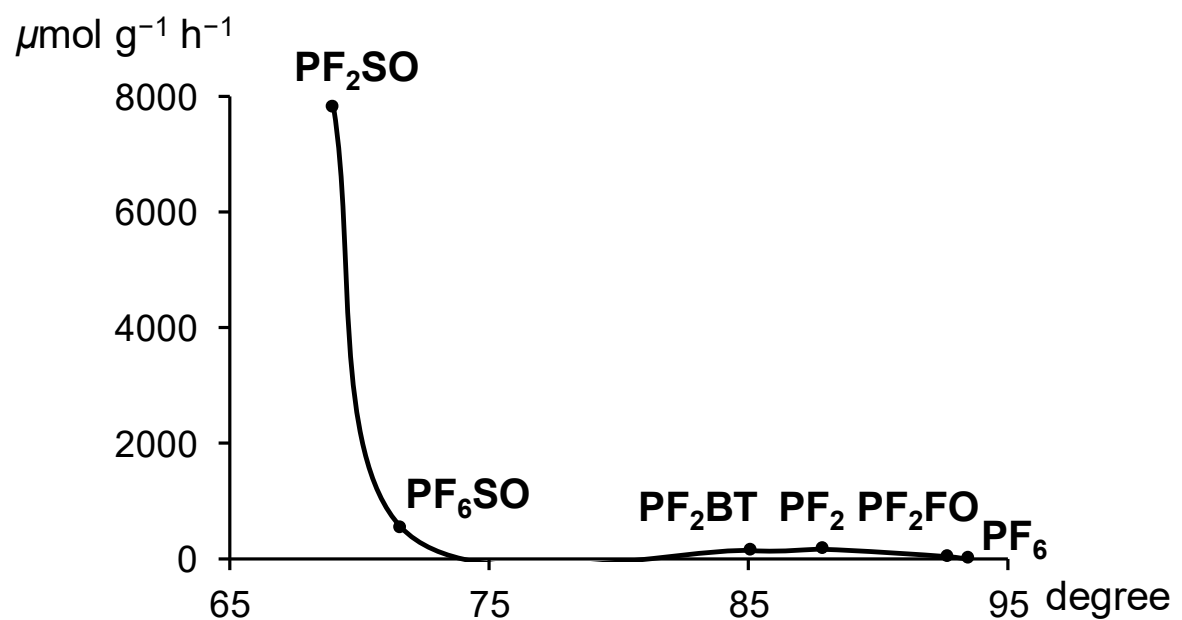


Figure S10. Plotting the average HER rate against the WCA for all polymers including **PF₂SO**.

10. Comparison of PF₂SO and PF₂BT with their analogues in terms of HER rate

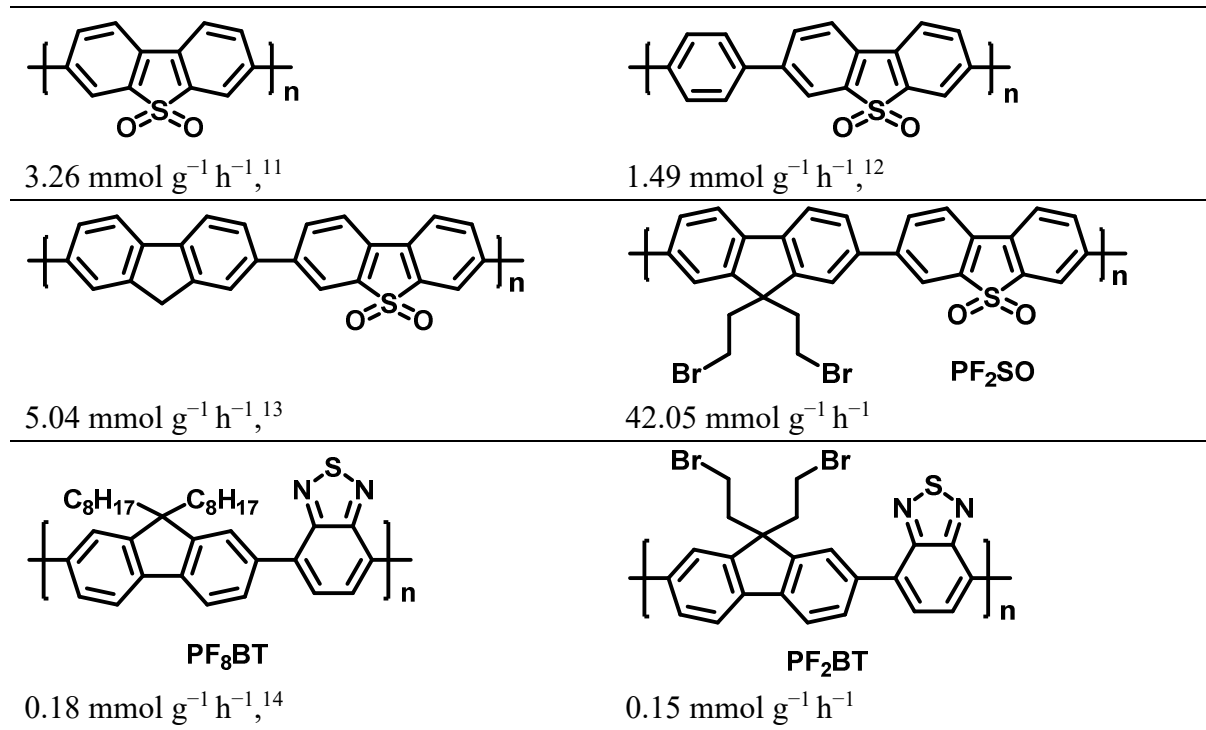


Figure S11. Comparison of PF₂SO and PF₂BT with their analogues in terms of HER rate.

11. NMR spectra

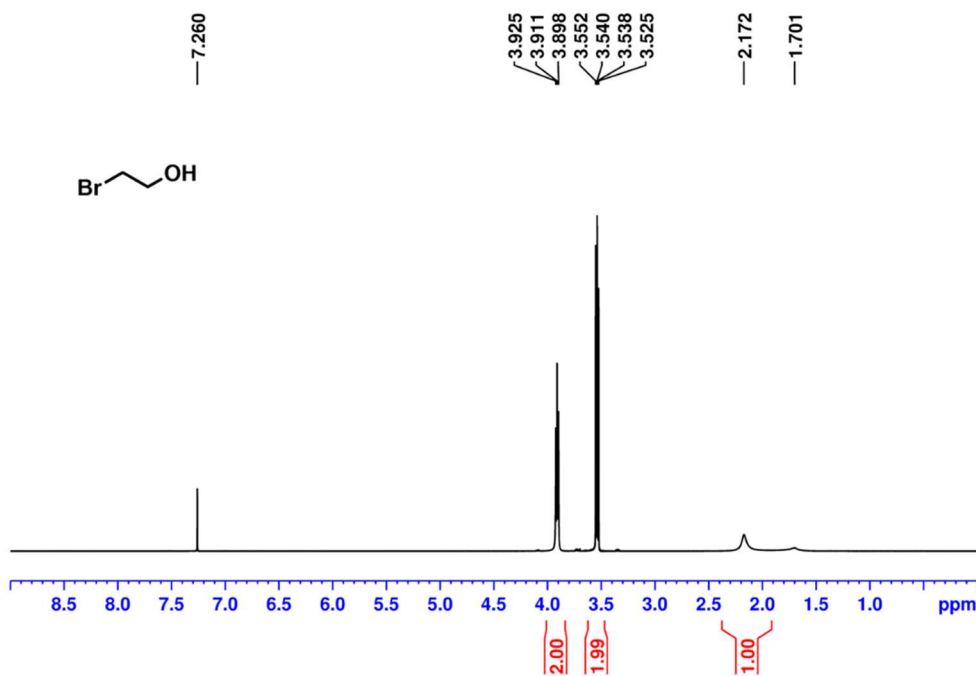


Figure S12. ^1H NMR spectrum of 2-bromoethanol (**1**) in CDCl_3 .

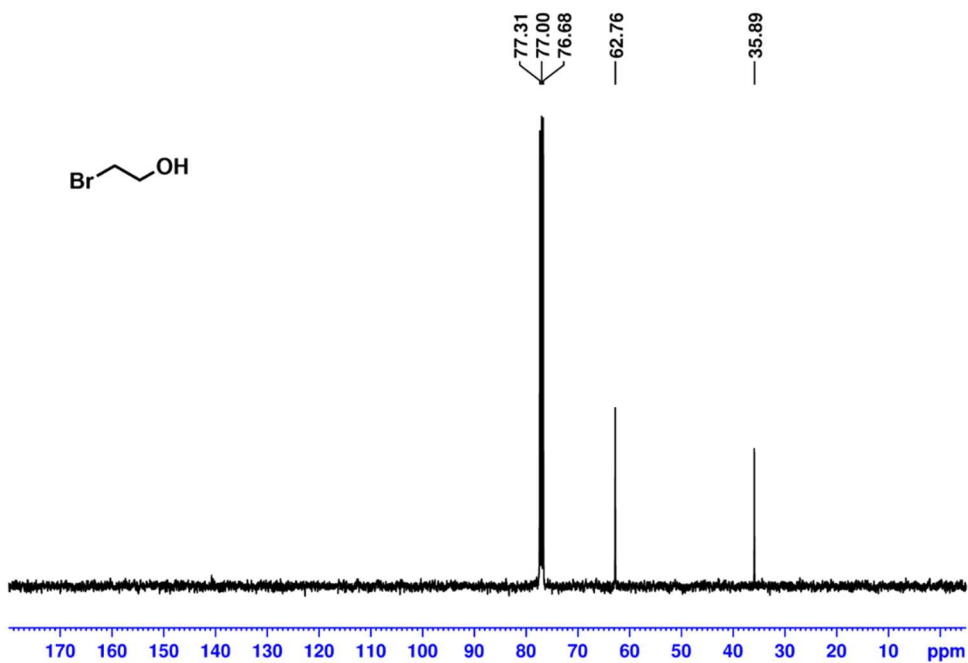


Figure S13. ^{13}C NMR spectrum of 2-bromoethanol (**1**) in CDCl_3 .

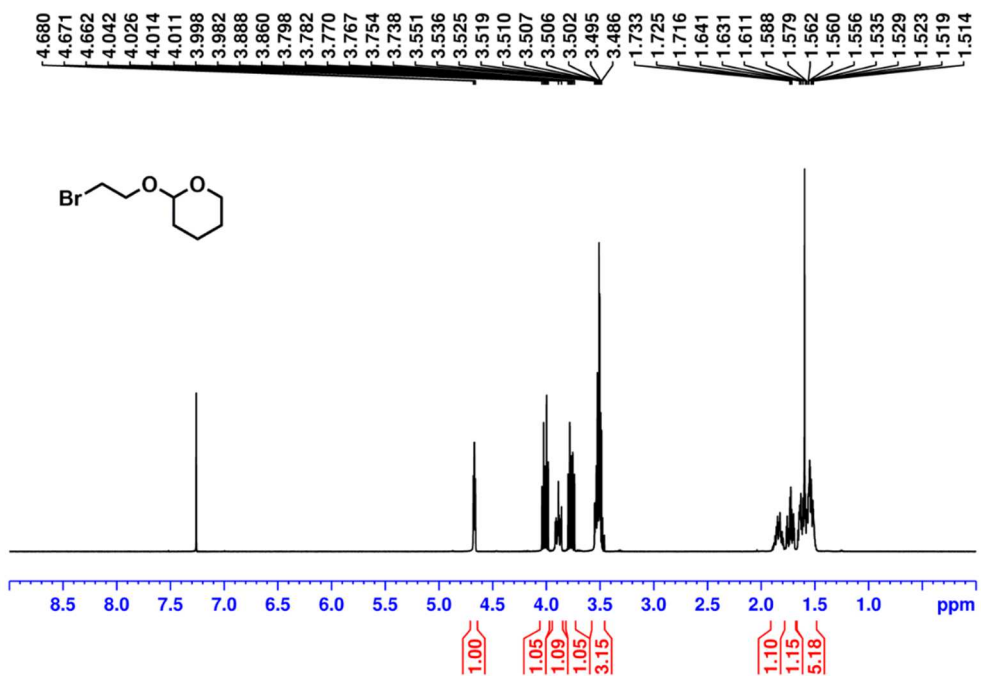


Figure S14. ¹H NMR spectrum of 2-(2-bromoethoxy)tetrahydro-2H-pyran (**2**) in CDCl₃.

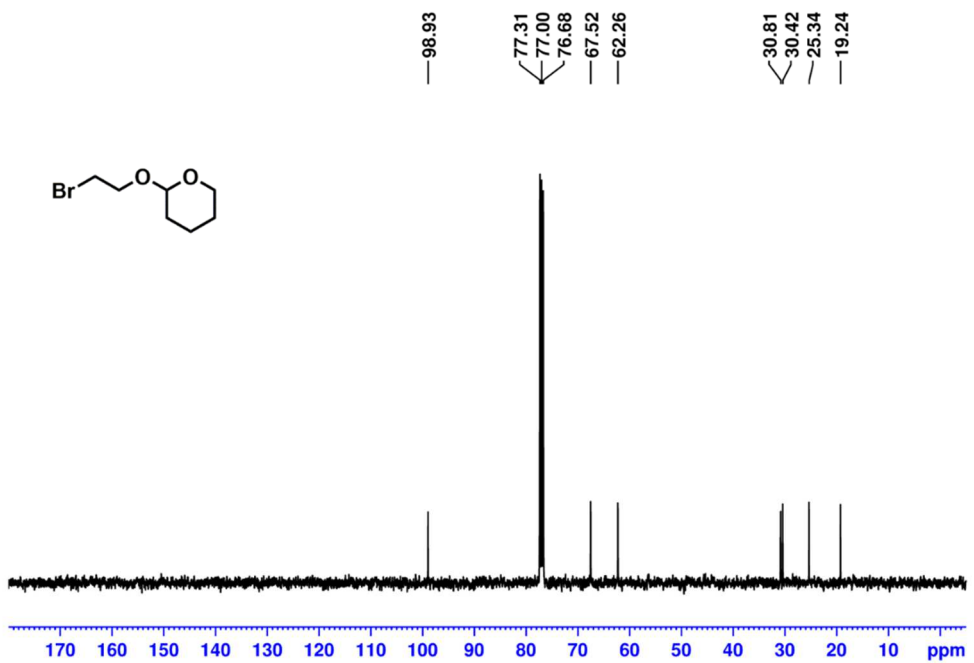


Figure S15. ¹³C NMR spectrum of 2-(2-bromoethoxy)tetrahydro-2H-pyran (**2**) in CDCl₃.

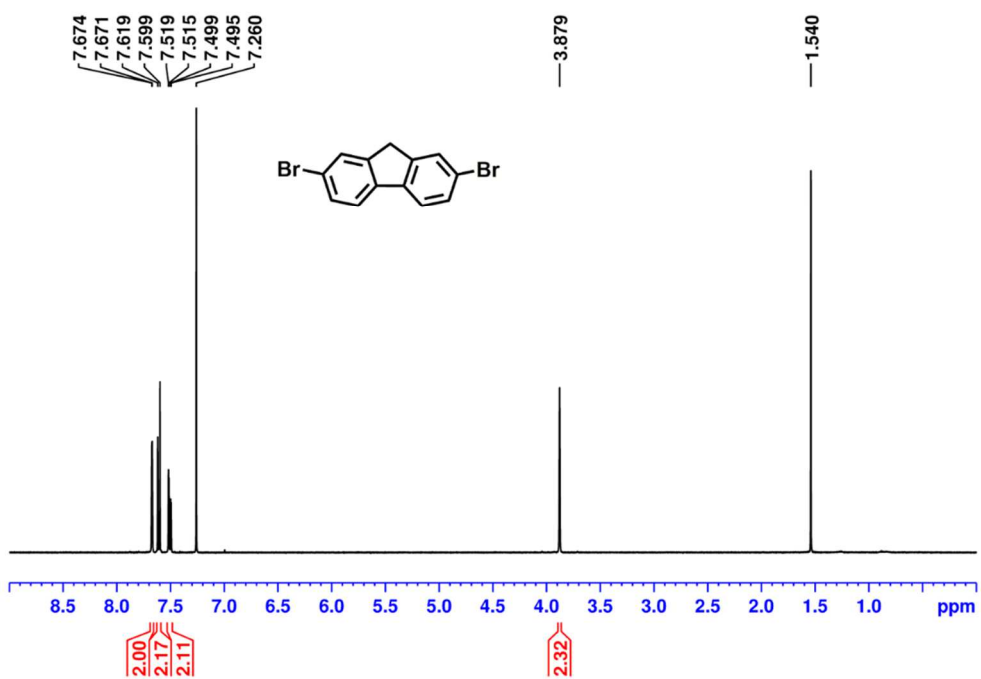


Figure S16. ^1H NMR spectrum of 2,7-dibromofluorene (**3**) in CDCl_3 .

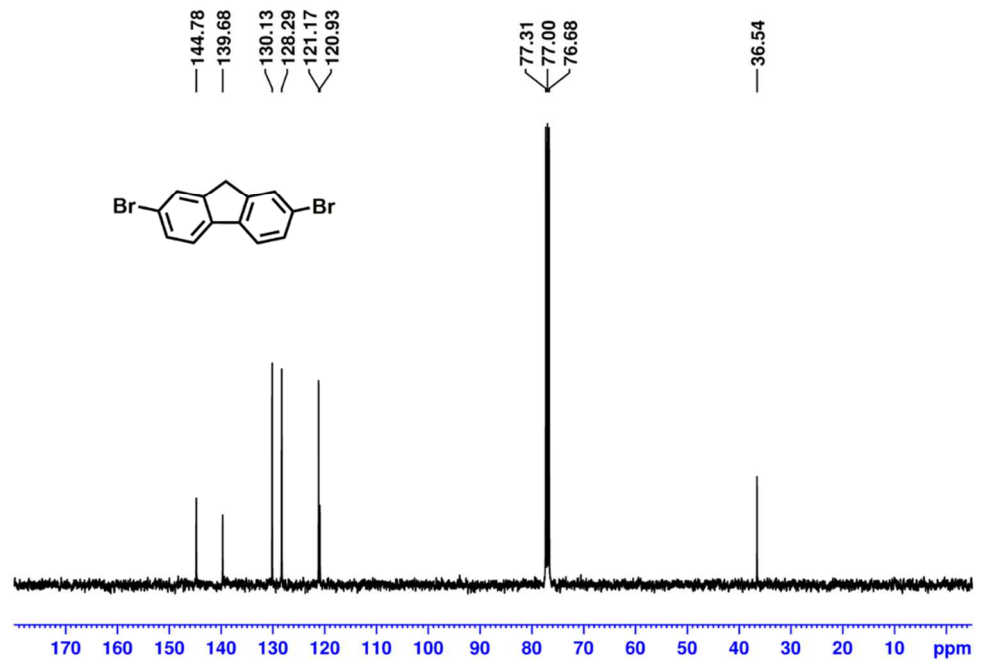


Figure S17. ^{13}C NMR spectrum of 2,7-dibromofluorene (**3**) in CDCl_3 .

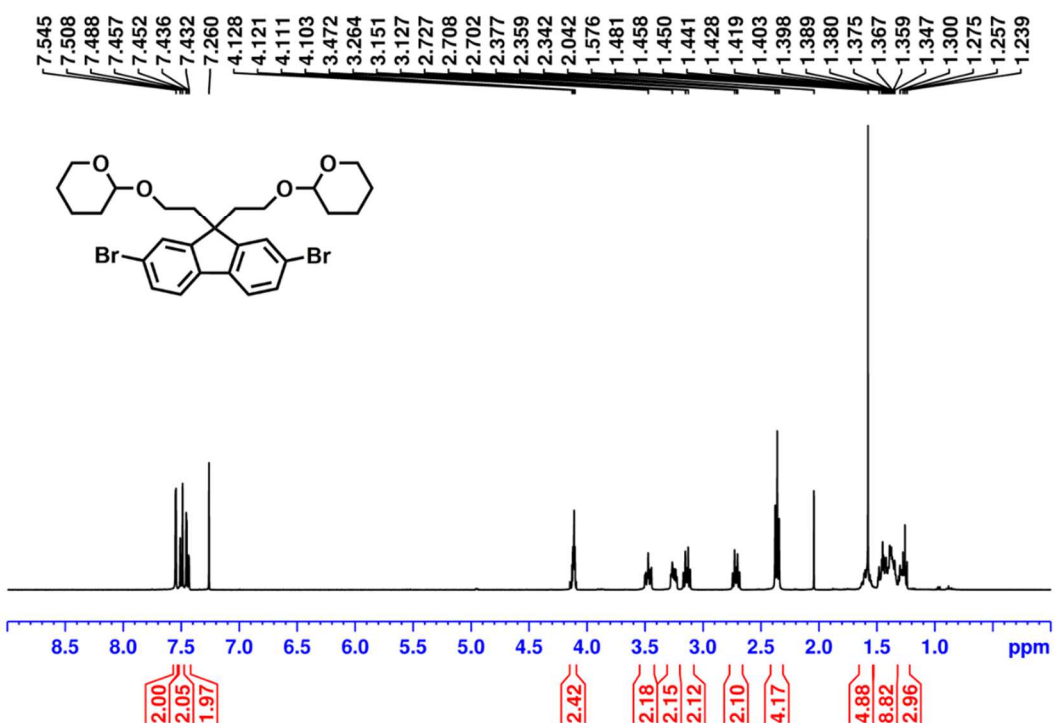


Figure S18. ¹H NMR spectrum of 2,2'-[^(2,7-dibromo-9H-fluoren-9-ylidene)bis(2,1-ethanediyoxy)]bis[tetrahydro-2H-pyran] (**4**) in CDCl₃

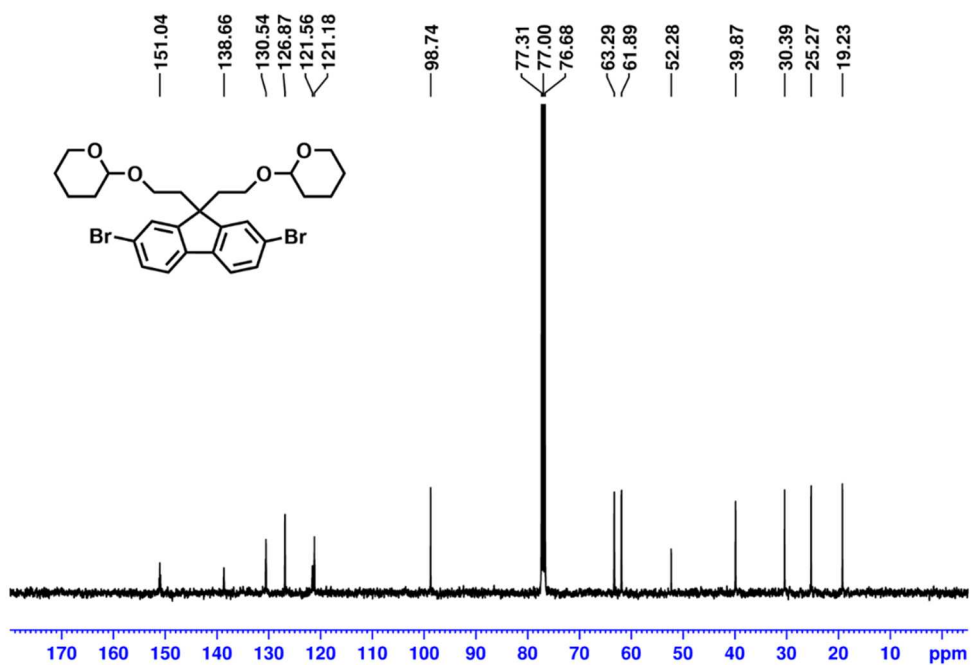


Figure S19. ¹³C NMR spectrum of 2,2'-[^(2,7-dibromo-9H-fluoren-9-ylidene)bis(2,1-ethanediyoxy)]bis[tetrahydro-2H-pyran] (**4**) in CDCl₃.

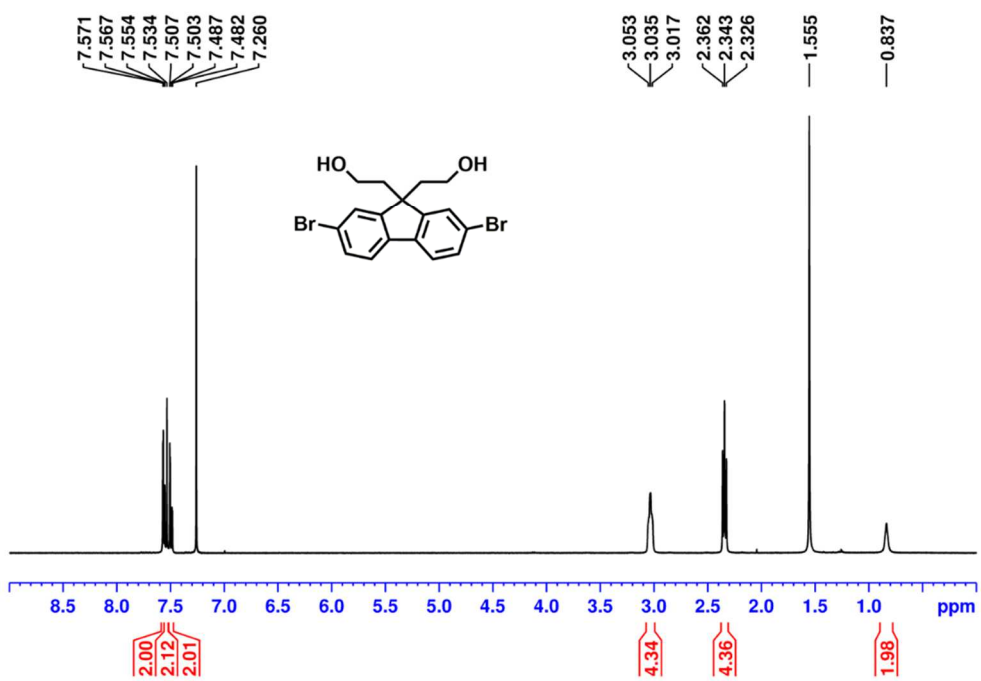


Figure S20. ^1H NMR spectrum of 2,7-dibromo-9H-fluorene-9,9-diethanol (**5**) in CDCl_3 .

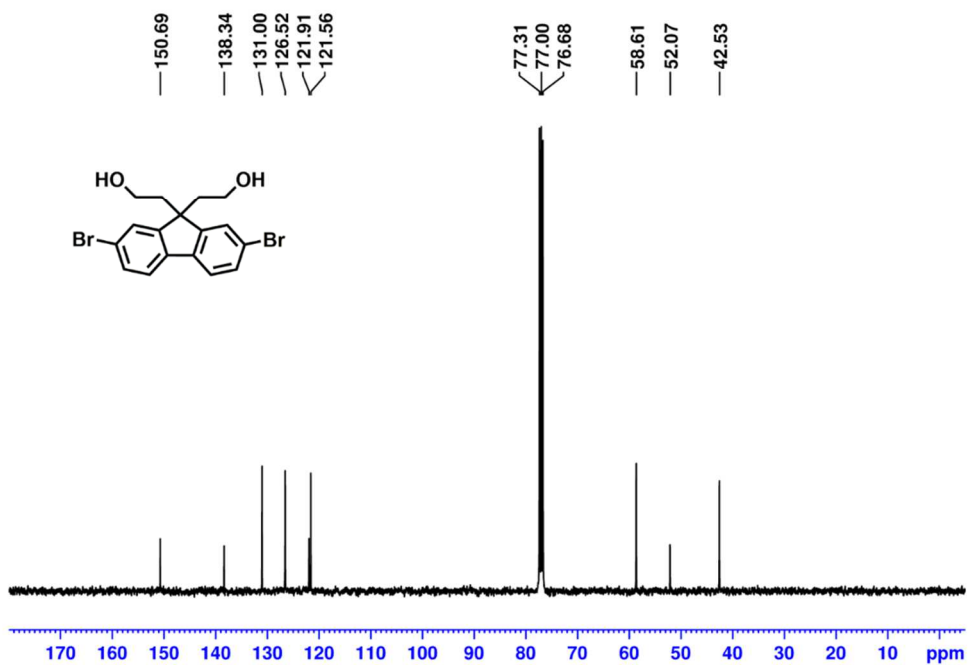


Figure S21. ^{13}C NMR spectrum of 2,7-dibromo-9H-fluorene-9,9-diethanol (**5**) in CDCl_3 .

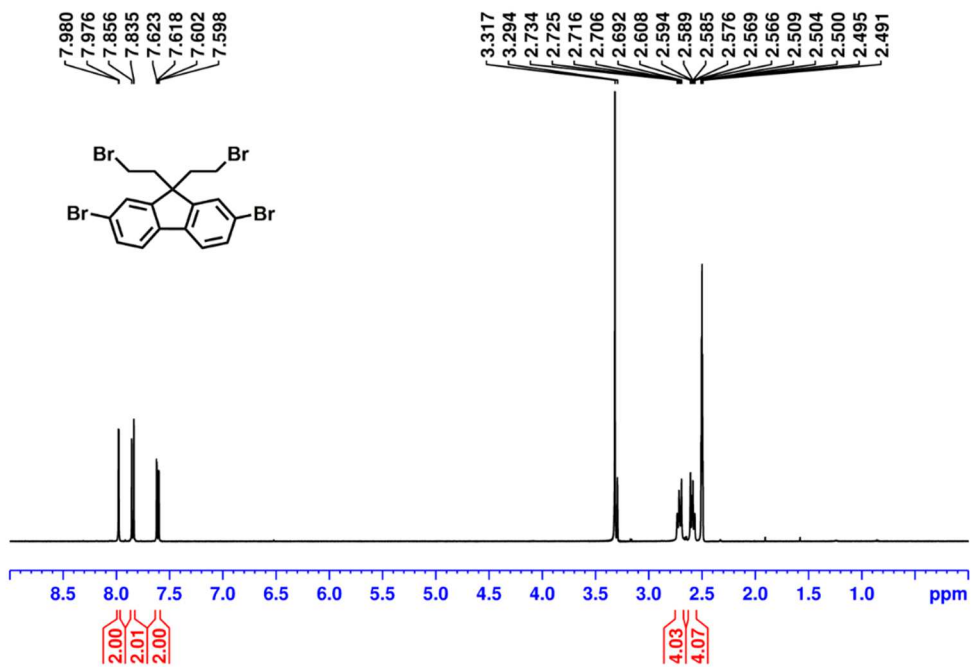


Figure S22. ^1H NMR spectrum of 2,7-dibromo-9,9-bis(2-bromoethyl)-9H-fluorene (**6**) in $\text{DMSO}-d_6$.

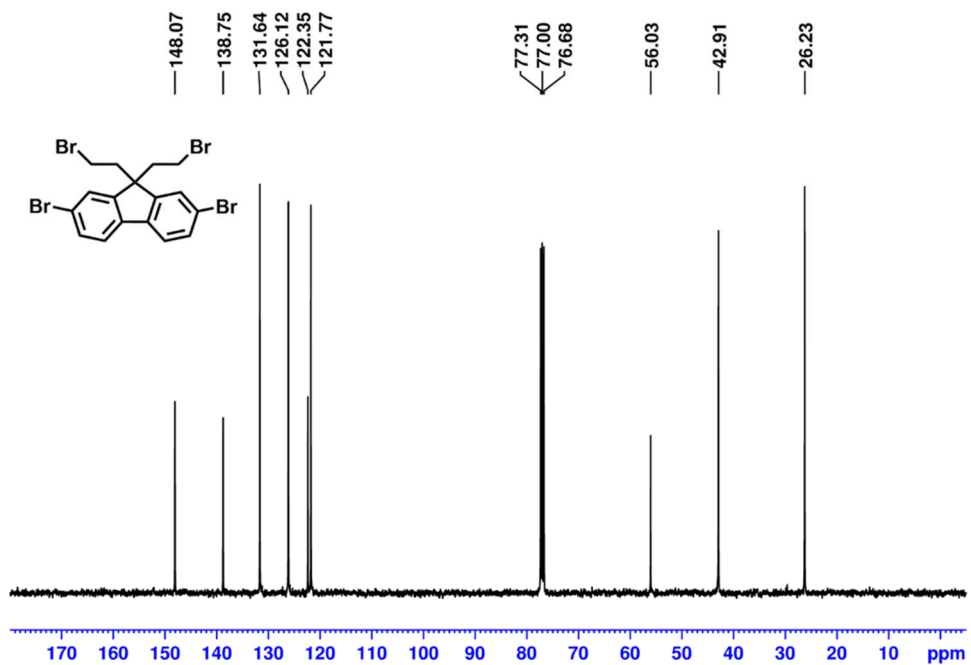


Figure S23. ^{13}C NMR spectrum of 2,7-dibromo-9,9-bis(2-bromoethyl)-9H-fluorene (**6**) in CDCl_3 .

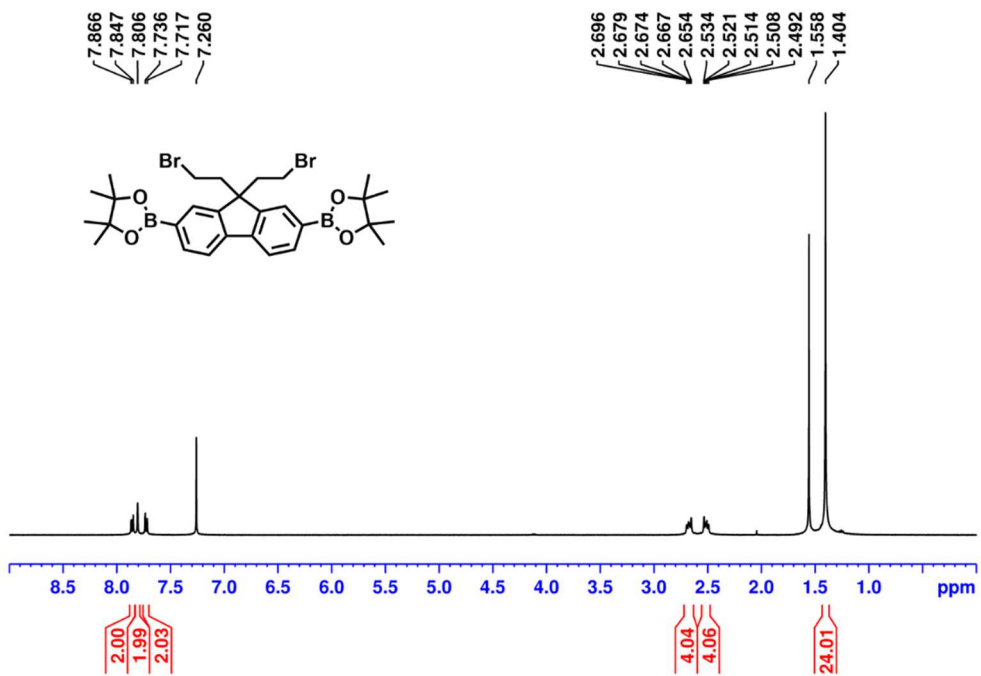


Figure S24. ^1H NMR spectrum of 2,2'-[9,9-bis(2-bromoethyl)-9H-fluorene-2,7-diyl]bis[4,4,5,5-tetramethyl-1,3,2-dioxaborolane] (7) in CDCl_3 .

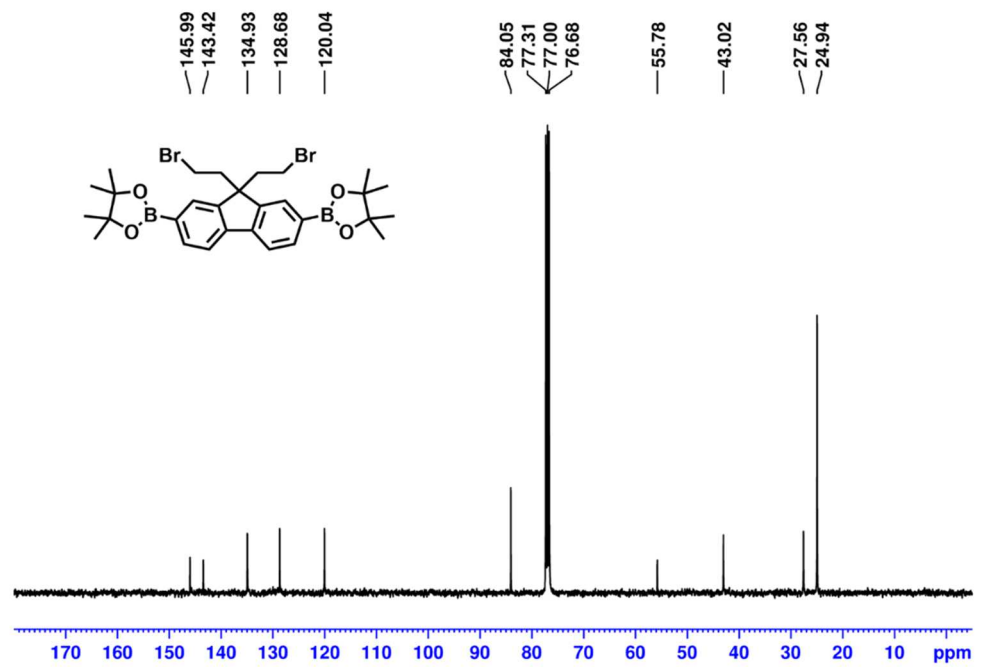


Figure S25. ^{13}C NMR spectrum of 2,2'-[9,9-bis(2-bromoethyl)-9H-fluorene-2,7-diyl]bis[4,4,5,5-tetramethyl-1,3,2-dioxaborolane] (7) in CDCl_3 .

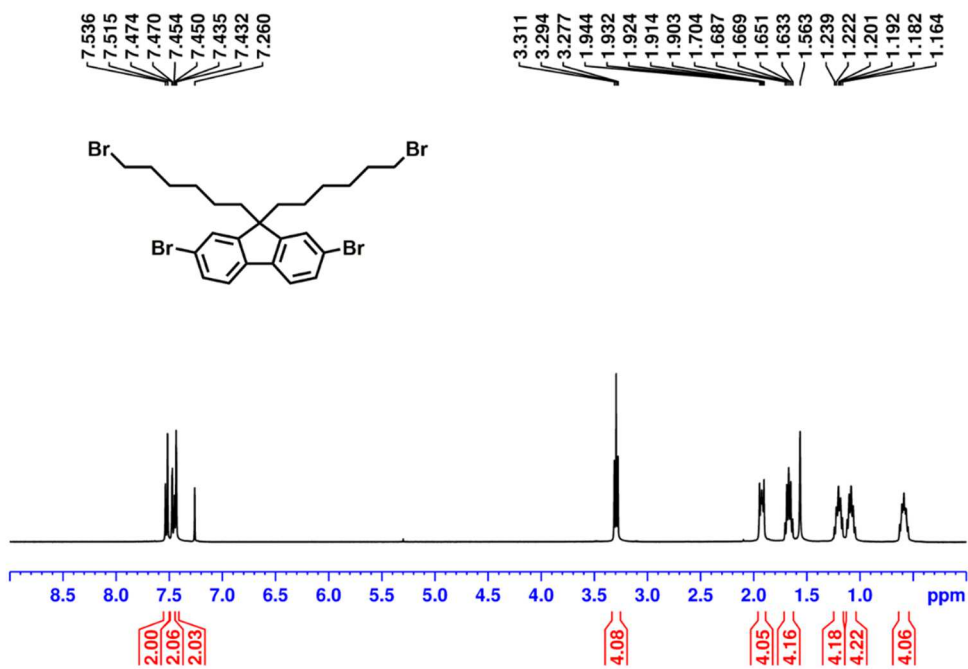


Figure S26. ¹H NMR spectrum of 2,7-dibromo-9,9-bis(6-bromohexyl)-9H-fluorene (**8**) in CDCl₃.

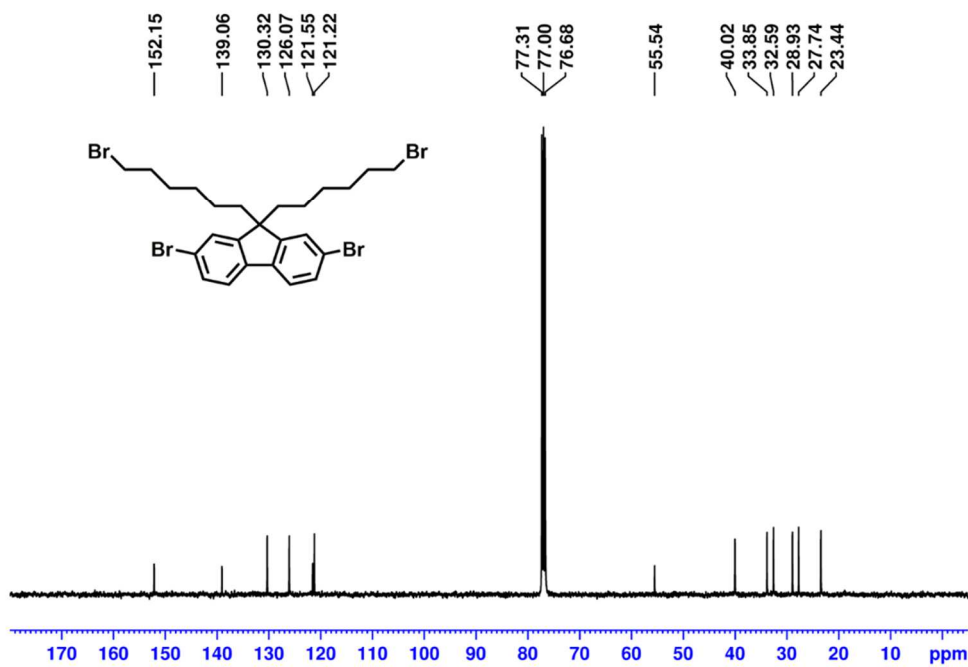


Figure S27. ¹³C NMR spectrum of 2,7-dibromo-9,9-bis(6-bromohexyl)-9H-fluorene (**8**) in CDCl₃.

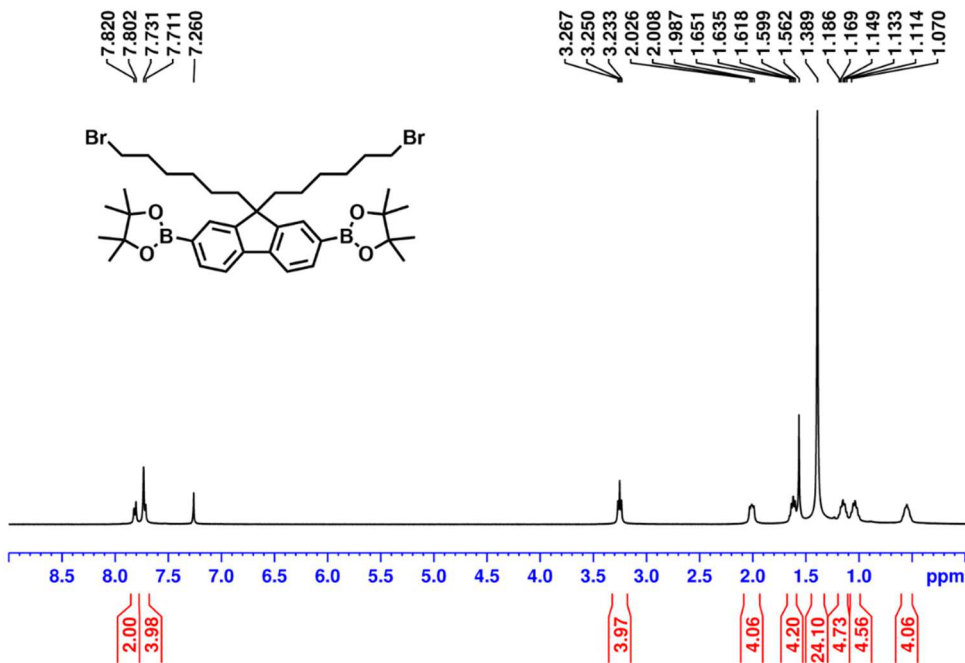


Figure S28. ^1H NMR spectrum of 2,2'-[9,9-bis(6-bromohexyl)-9H-fluorene-2,7-diyl]bis[4,4,5,5-tetramethyl-1,3,2-dioxaborolane] (**9**) in CDCl_3 .

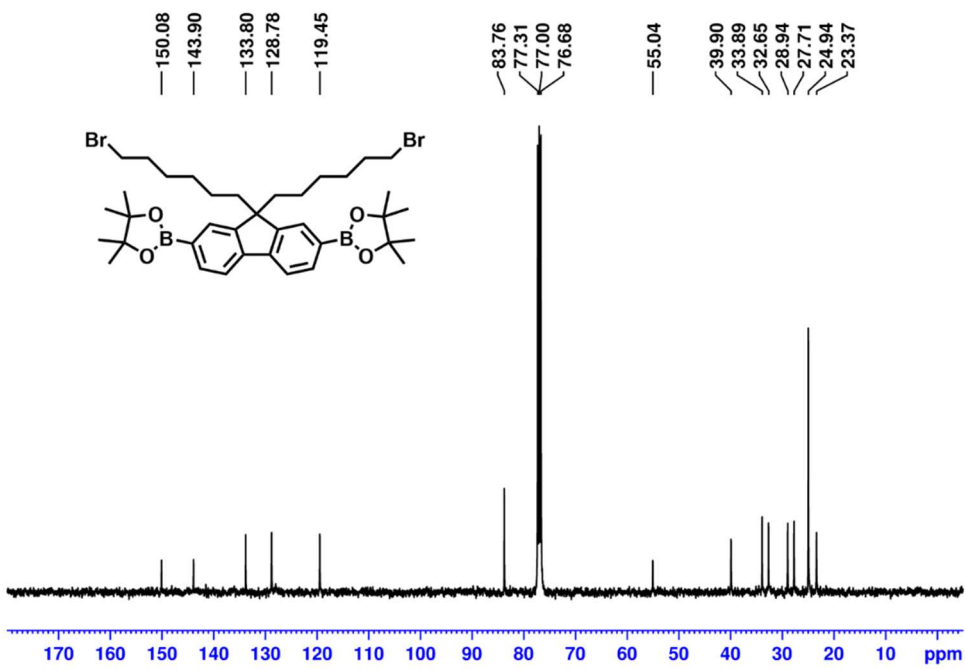


Figure S29. ^{13}C NMR spectrum of 2,2'-[9,9-bis(6-bromohexyl)-9H-fluorene-2,7-diyl]bis[4,4,5,5-tetramethyl-1,3,2-dioxaborolane] (**9**) in CDCl_3 .

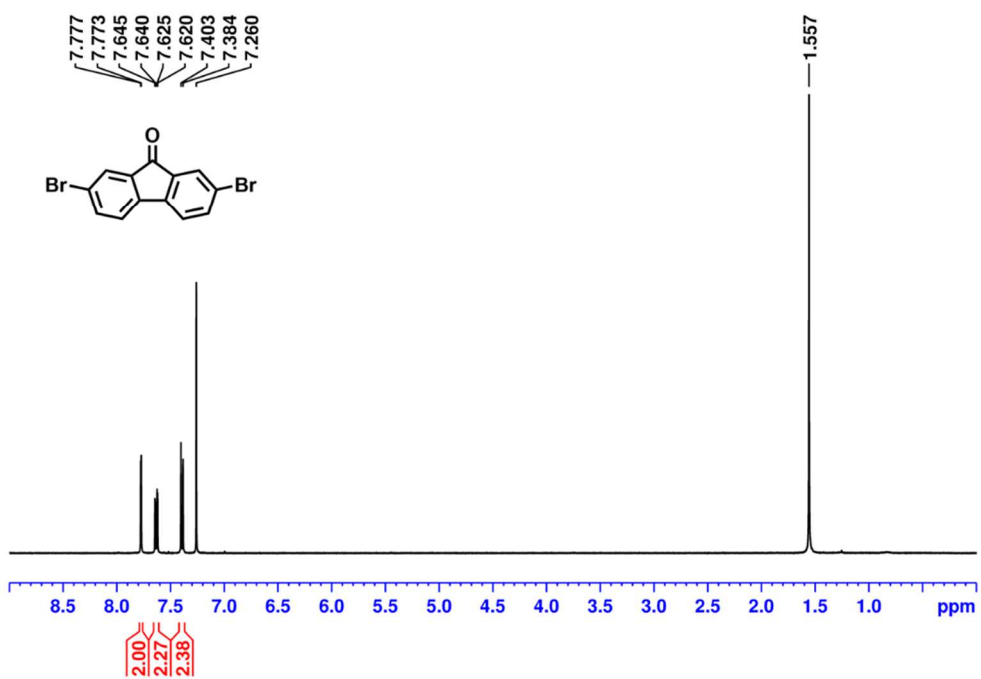


Figure S30. ^1H NMR spectrum of 2,7-dibromo-9-fluorenone (**10**) in CDCl_3 .

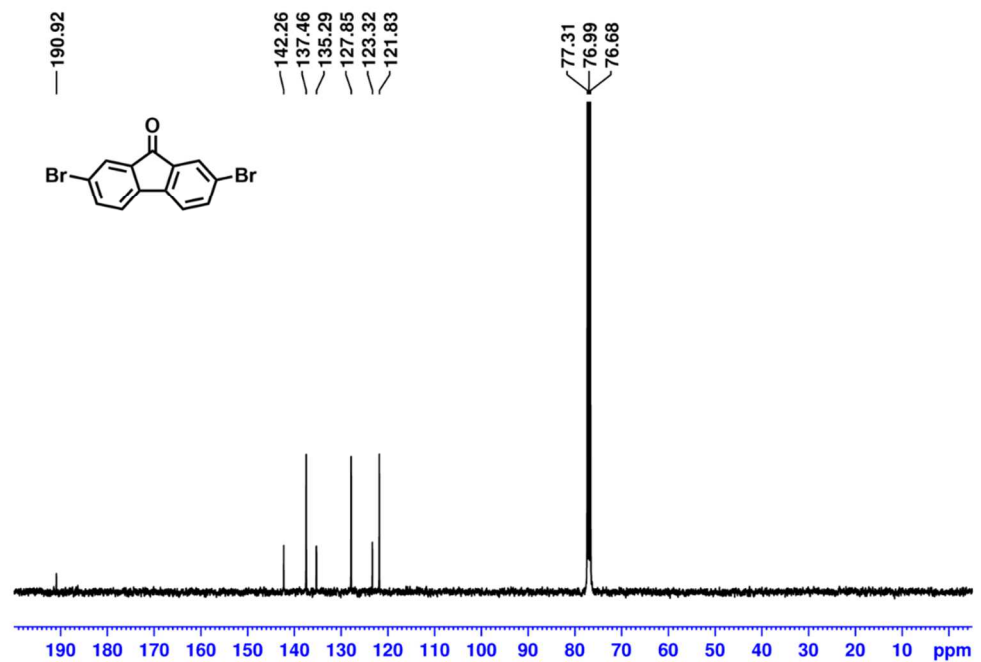


Figure S31. ^{13}C NMR spectrum of 2,7-dibromo-9-fluorenone (**10**) in CDCl_3 .

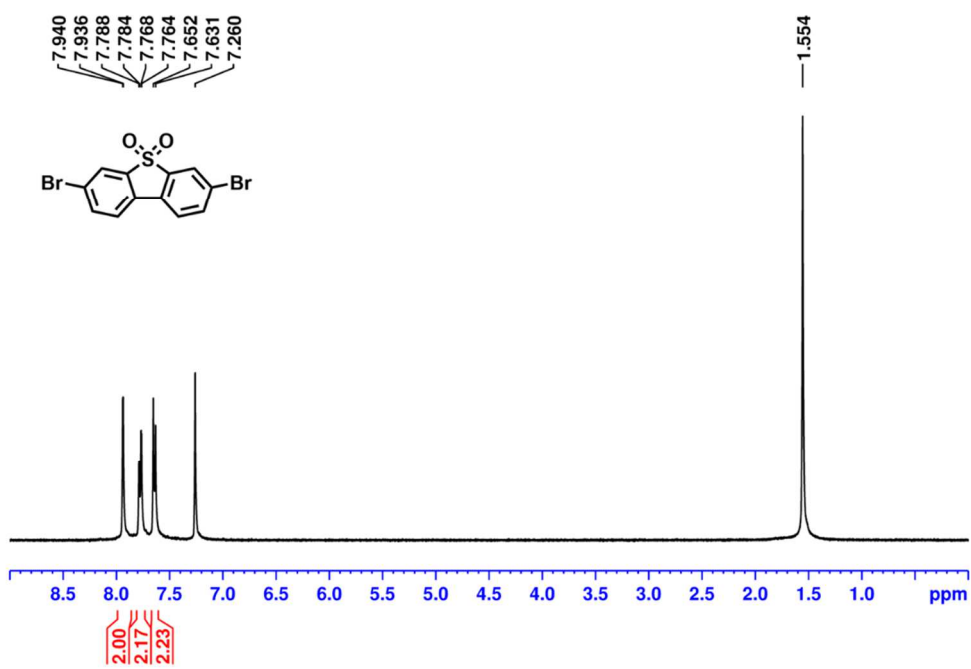


Figure S32. ^1H NMR spectrum of 3,7-dibromodibenzothiophene S,S-dioxide (**11**) in CDCl_3 .

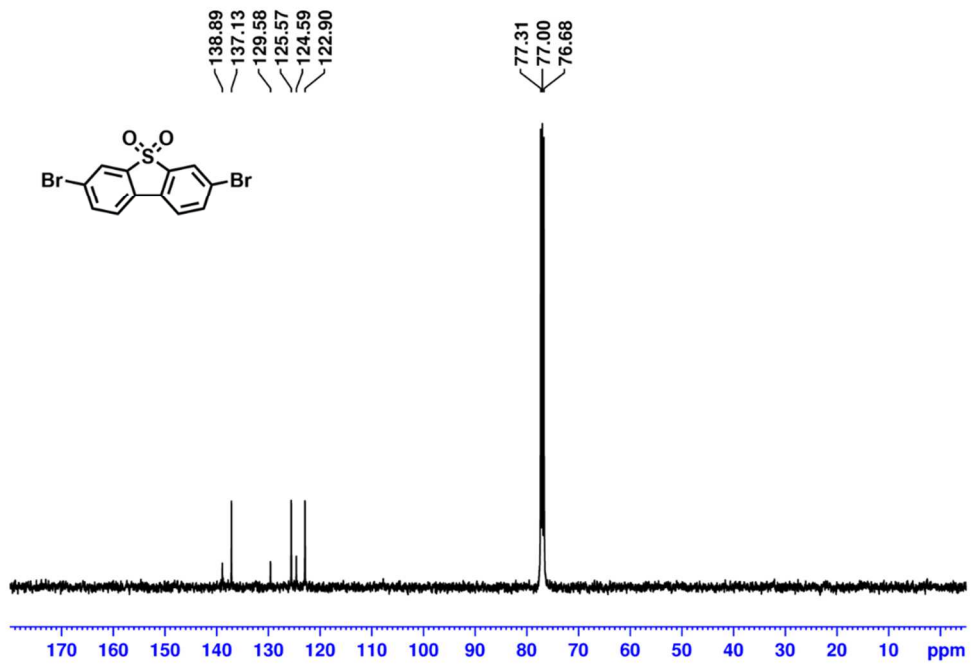


Figure S33. ^{13}C NMR spectrum of 3,7-dibromodibenzothiophene S,S-dioxide (**11**) in CDCl_3 .

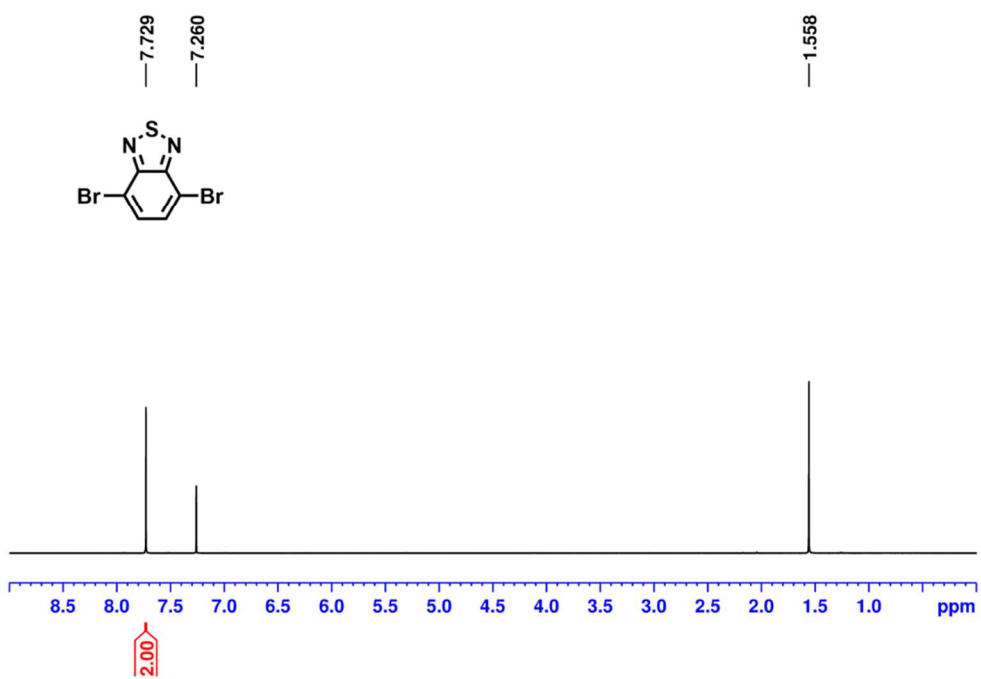


Figure S34. ¹H NMR spectrum of 4,7-dibromo-2,1,3-benzothiadiazole (**12**) in CDCl₃.

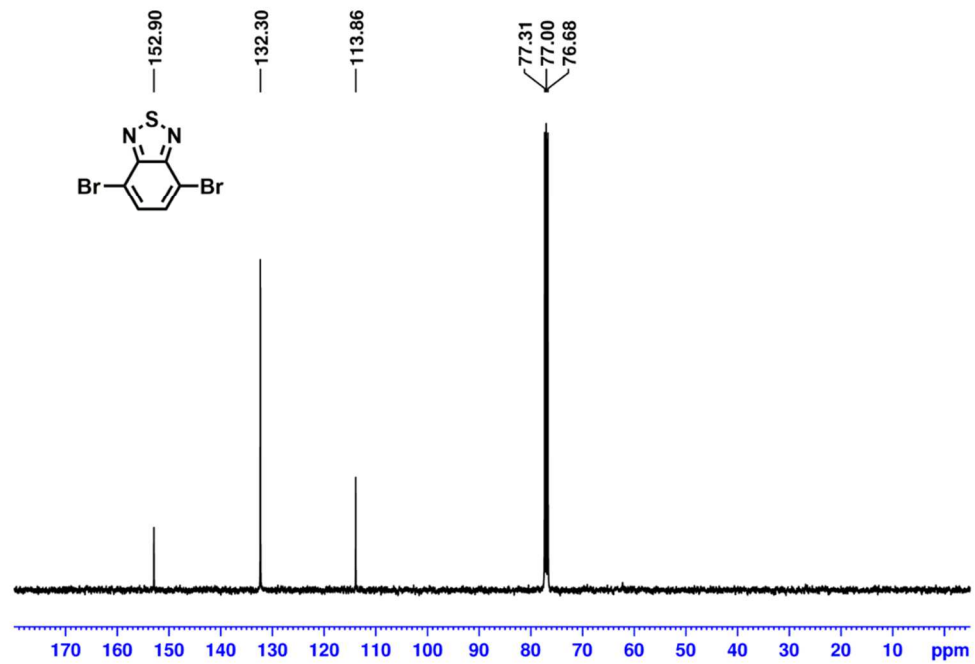


Figure S35. ¹³C NMR spectrum of 4,7-dibromo-2,1,3-benzothiadiazole (**12**) in CDCl₃.

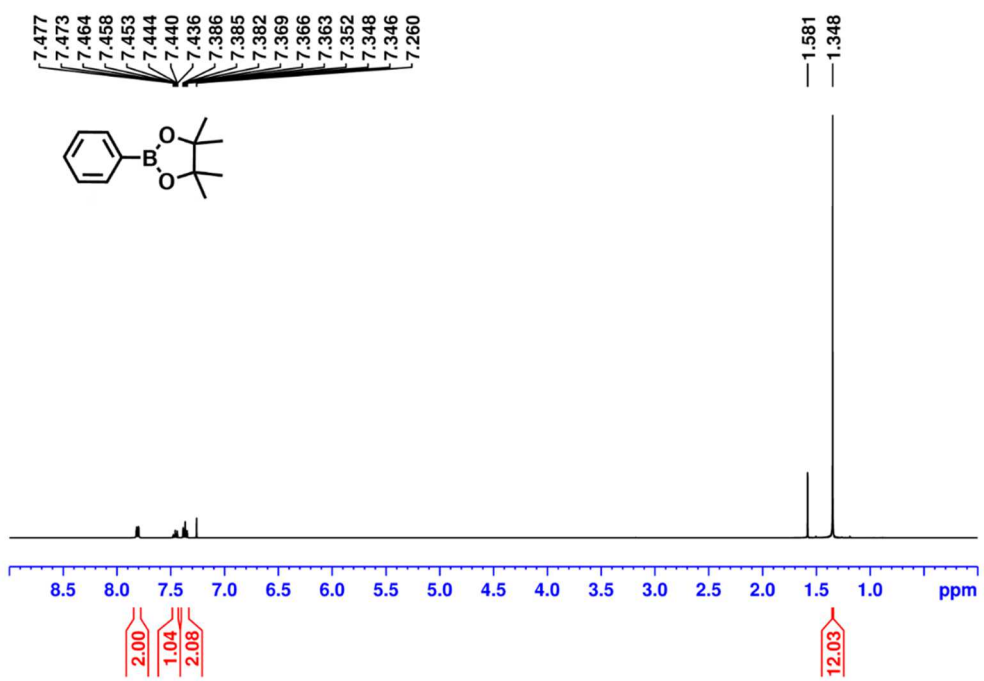


Figure S36. ^1H NMR spectrum of phenylboronic acid pinacol ester in CDCl_3 .

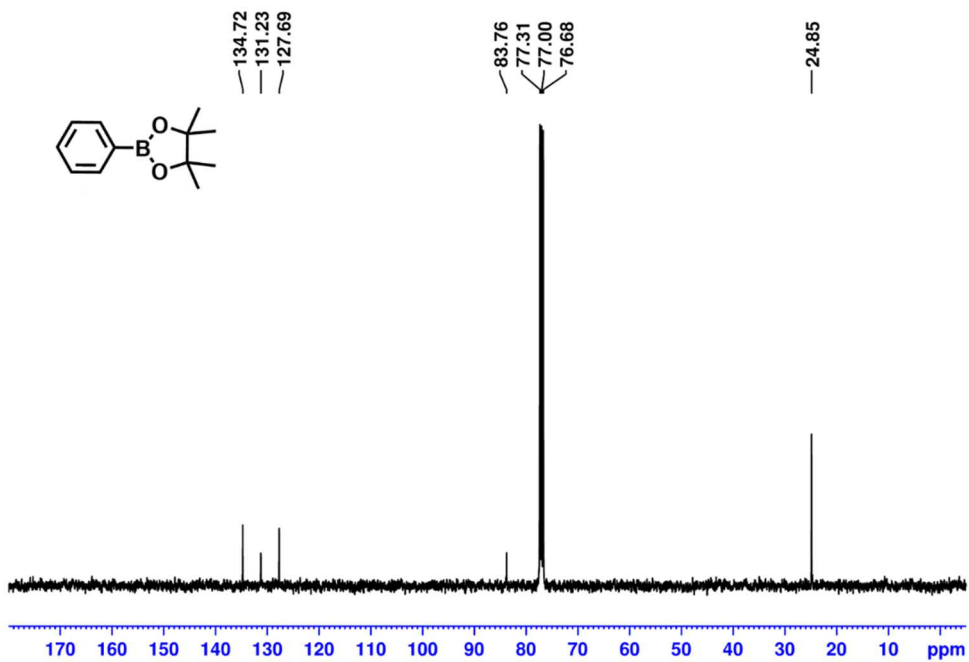


Figure S37. ^{13}C NMR spectrum of phenylboronic acid pinacol ester in CDCl_3 .

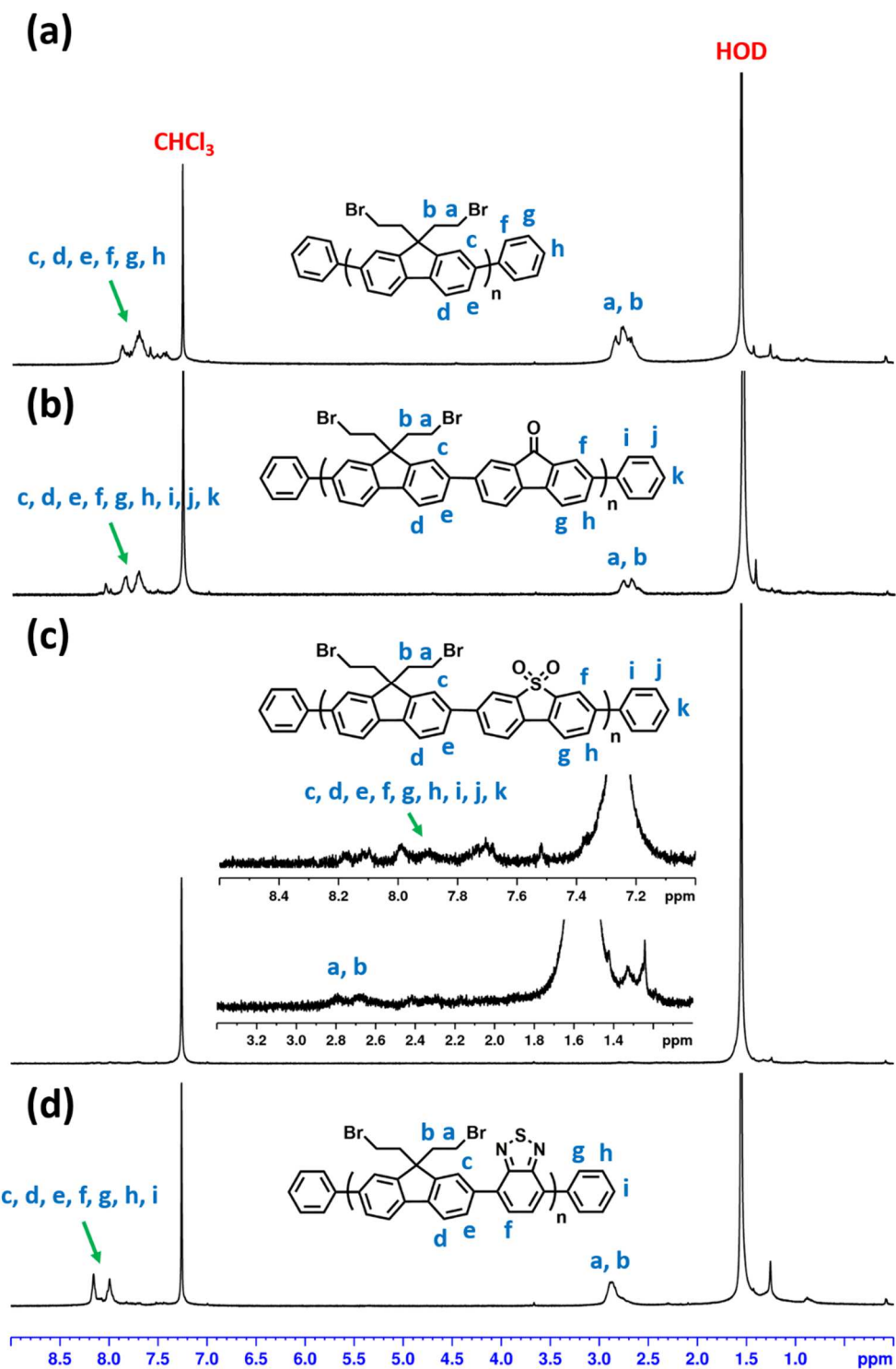


Figure S38. ¹H NMR spectra of (a) PF₂, (b) PF₂FO, (c) PF₂SO, and (d) PF₂BT.

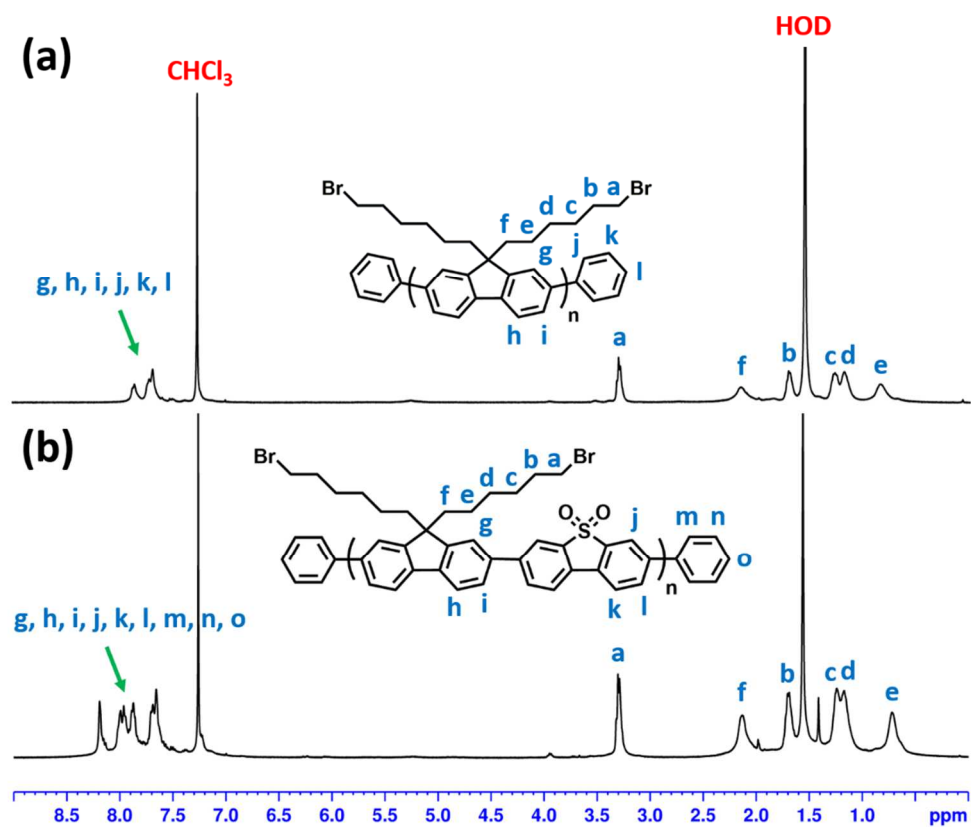
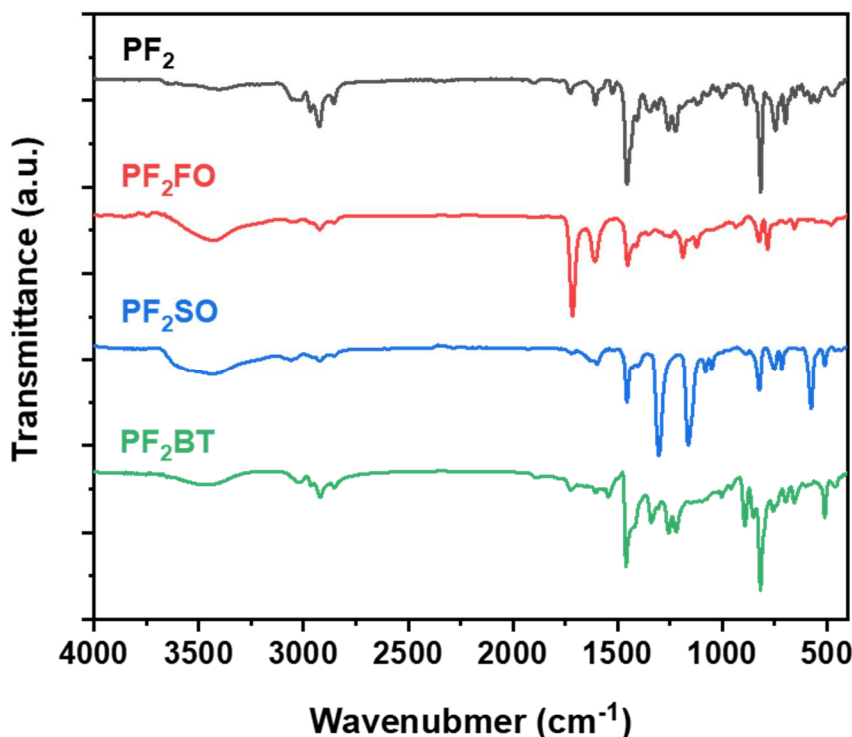


Figure S39. ¹H NMR spectra (a) PF₆ and (b) PF₆SO.

12. IR spectra



PF₂, FT-IR (KBr, cm⁻¹): 698, 745, 817 (aromatic sp² C-H out-of-plane bending); 1221, 1257 (alkyl C-H wagging, (-CH₂Br)); 1406, 1438, 1454, 1523, 1569, 1604 (aromatic C-C stretching (in ring)); 2855, 2924, 2966 (alkyl sp³ C-H stretching); 3007, 3028, 3055 (aromatic sp² C-H stretching).

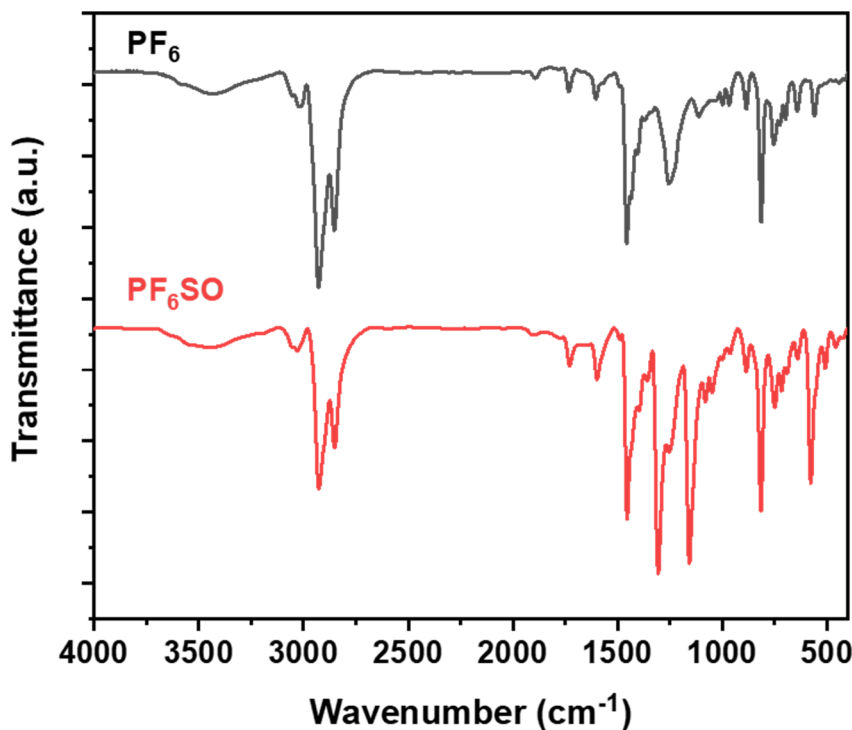
PF₂FO, FT-IR (KBr, cm⁻¹): 655, 784, 824 (aromatic sp² C-H out-of-plane bending); 1122, 1188 (alkyl C-H wagging, (-CH₂Br)); 1410, 1452, 1608 (aromatic C-C stretching (in ring)); 1715 (C=O stretching); 2851, 2923 (alkyl sp³ C-H stretching); 3047 (aromatic sp² C-H stretching).

PF₂SO, FT-IR (KBr, cm⁻¹): 576 (alkyl C-Br stretching, (-CH₂Br)); 715, 750, 823 (aromatic sp² C-H out-of-plane bending); 1050, 1079 (alkyl C-H wagging, (-CH₂Br)); 1163 (symmetric S=O stretching); 1302 (asymmetric S=O stretching); 1405, 1456, 1597 (aromatic C-C stretching (in ring)); 2852, 2922 (alkyl sp³ C-H stretching); 3034, 3059, 3083 (aromatic sp² C-H stretching).

PF₂BT, FT-IR (KBr, cm⁻¹): 511 (alkyl C-Br stretching, (-CH₂Br)); 657, 697, 817 (aromatic sp² C-H out-of-plane bending); 1220, 1256 (alkyl C-H wagging, (-CH₂Br)); 1418, 1459, 1544, 1604 (aromatic C-C stretching (in ring)); 2851, 2919, 2962 (alkyl sp³ C-H stretching); 3008,

3028, 3053 (aromatic sp² C-H stretching).

Figure S40. FT-IR spectra of **PF₂**, **PF₂FO**, **PF₂SO**, and **PF₂BT**.



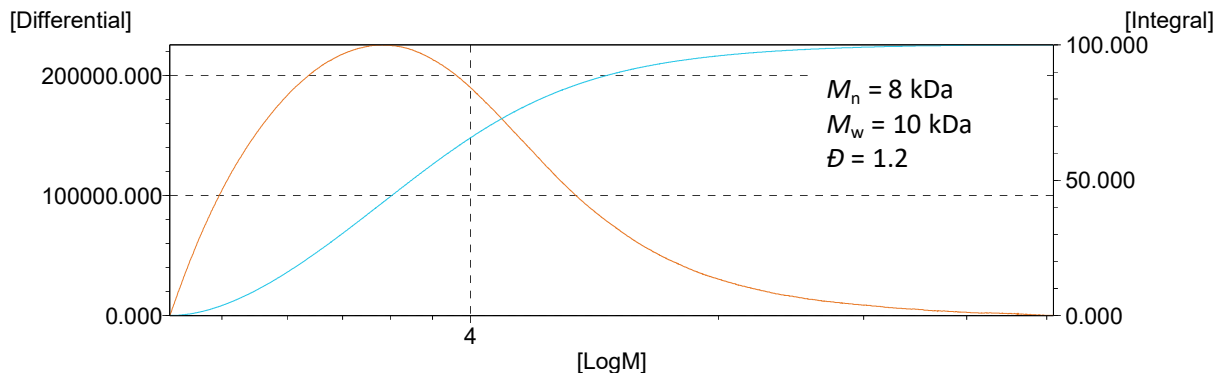
PF₆, FT-IR (KBr, cm⁻¹): 560 (alkyl C-Br stretching, (-CH₂Br)); 724, 754, 814 (aromatic sp² C-H out-of-plane bending); 1255 (alkyl C-H wagging, (-CH₂Br)); 1404, 1436, 1456, 1568, 1604 (aromatic C-C stretching (in ring)); 2852, 2927 (alkyl sp³ C-H stretching); 3008, 3023, 3055 (aromatic sp² C-H stretching).

PF₆SO, FT-IR (KBr, cm⁻¹): 577 (alkyl C-Br stretching, (-CH₂Br)); 716, 750, 816 (aromatic sp² C-H out-of-plane bending); 1048, 1080 (alkyl C-H wagging, (-CH₂Br)); 1157 (symmetric S=O stretching); 1306 (asymmetric S=O stretching); 1397, 1431, 1454, 1597 (aromatic C-C stretching (in ring)); 2851, 2925 (alkyl sp³ C-H stretching); 3028, 3053 (aromatic sp² C-H stretching).

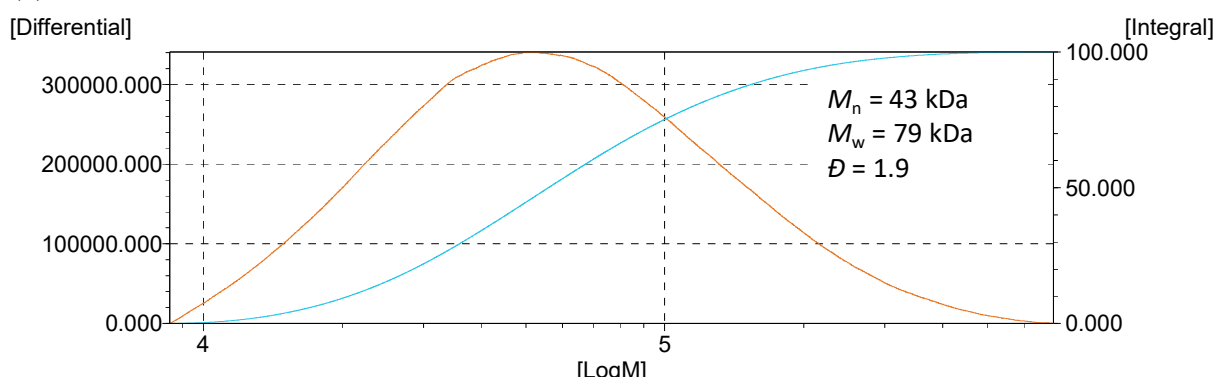
Figure S41. FT-IR spectra of **PF₆** and **PF₆SO**.

13. GPC traces

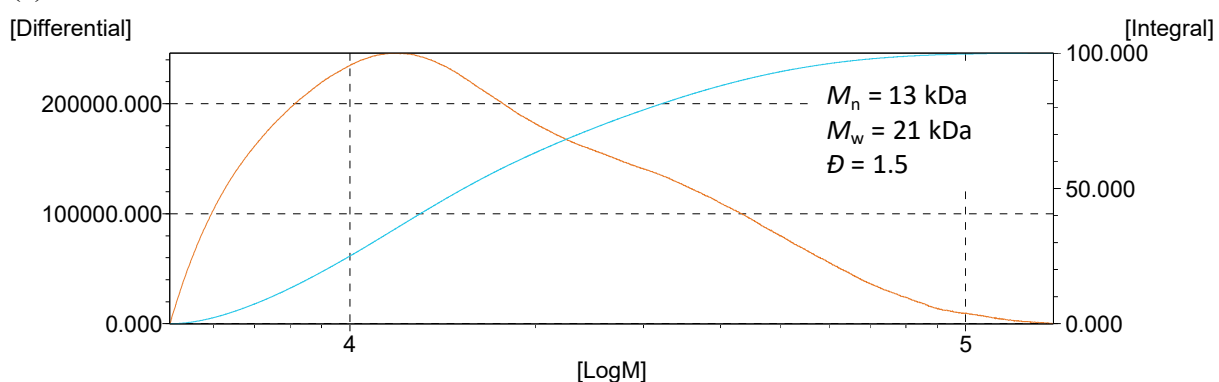
(a) PF₂



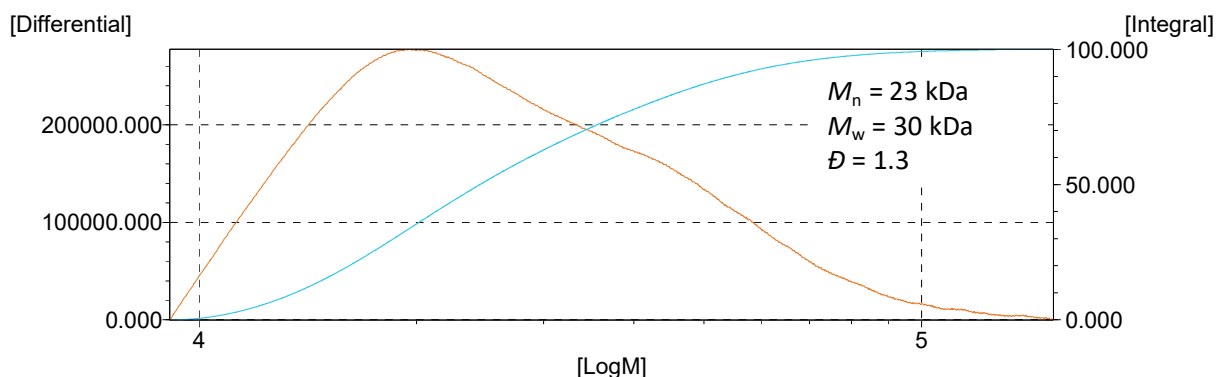
(b) PF₆



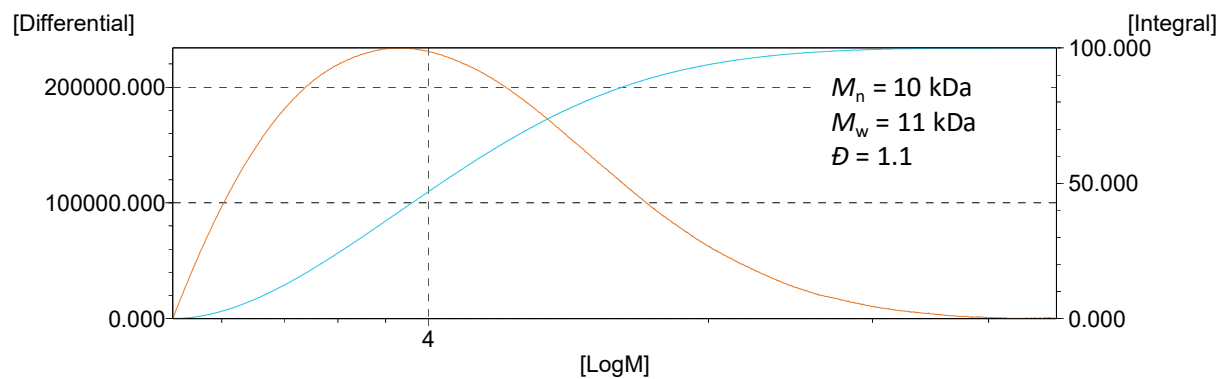
(c) PF₆SO



(d) PF₂BT



(e) PF₂FO



14. Reference

- 1 S. Ranganathan, D. Ranganathan and S. K. Singh, *Tetrahedron Lett.*, 1987, **28**, 2893-2894.
- 2 J. A. Murphy, M. Mahesh, G. McPheator, R. V. Anand, T. M. McGuire, R. Carling and A. R. Kennedy, *Org. Lett.*, 2007, **9**, 3233-3236.
- 3 D. W. Price and J. M. Tour, *Tetrahedron*, 2003, **59**, 3131-3156.
- 4 J. Lee, H.-J. Cho, B.-J. Jung, N. S. Cho and H.-K. Shim, *Macromolecules*, 2004, **37**, 8523-8529.
- 5 D. Stay and M. C. Lonergan, *Macromolecules*, 2013, **46**, 4361-4369.
- 6 B. Liu and S. K. Dishari, *Chem. Eur. J.*, 2008, **14**, 7366-7375.
- 7 D. M. E. Freeman, A. J. Musser, J. M. Frost, H. L. Stern, A. K. Forster, K. J. Fallon, A. G. Rapidis, F. Cacialli, I. McCulloch, T. M. Clarke, R. H. Friend and H. Bronstein, *J. Am. Chem. Soc.*, 2017, **139**, 11073-11080.
- 8 A. Liang, M. Luo, Y. Liu, H. Wang, Z. Wang, X. Zheng, T. Cao, D. Liu, Y. Zhang and F. Huang, *Dyes Pigm*, 2018, **159**, 637-645.
- 9 H. Akpinar, A. Balan, D. Baran, E. K. Unver and L. Toppore, *Polymer*, 2010, **51**, 6123-6131.
- 10 D. C. Gerbino, S. D. Mandolesi, H.-G. Schmalz and J. C. Podestá, *Eur. J. Org. Chem.*, 2009, **2009**, 3964-3972.
- 11 M. Sachs, R. S. Sprick, D. Pearce, S. A. J. Hillman, A. Monti, A. A. Y. Guilbert, N. J. Brownbill, S. Dimitrov, X. Shi, F. Blanc, M. A. Zwijnenburg, J. Nelson, J. R. Durrant and A. I. Cooper, *Nat. Commun.*, 2018, **9**, 4968.
- 12 R. S. Sprick, B. Bonillo, R. Clowes, P. Guiglion, N. J. Brownbill, B. J. Slater, F. Blanc, M. A. Zwijnenburg, D. J. Adams and A. I. Cooper, *Angew. Chem. Int. Ed.*, 2018, **57**, 2520-2520.
- 13 C. Dai, S. Xu, W. Liu, X. Gong, M. Panahandeh-Fard, Z. Liu, D. Zhang, C. Xue, K. P. Loh and B. Liu, *Small*, 2018, **14**, 1801839.
- 14 J. Kosco, M. Sachs, R. Godin, M. Kirkus, L. Francas, M. Bidwell, M. Qureshi, D. Anjum, J. R. Durrant and I. McCulloch, *Adv. Energy Mater.*, 2018, **8**, 1802181.